Table 4. Reports of interstitial lung disease due to docetaxel plus gemcitabine regimen

Author	Year	Study type	Treatment schedule	*n*	Grades 3–4 ILD (%)	TRD (%)
Rebattu et al. [13]	2001	Phase I/II	Docetaxel (60, 75, 85, 100 mg/m^2) day 8; gemcitabine (1000 mg/m^2), days 1 and 8, every 3 weeks	49	3 (6.1)	0
Kouroussis et al. [25]	2004	Phase I	Docetaxel (30, 35, 40 mg/m^2), days 1, 8 and 15; gemcitabine (700, 800, 900, 1000 mg/m^2), days 1, 8 and 15, every 4 weeks	26	6 (23)	2 (7.7)
Matsui et al. [21]	2005	Phase I/II	Docetaxel (50, 60 mg/m^2) day 1 or 8; gemcitabine (800, 1000 mg/m^2), days 1 and 8, every 3 weeks	59	3 (5.1)	0
Pujor et al. [27]	2005	Phase III	Docetaxel (85 mg/m^2) day 8; gemcitabine (1000 mg/m^2), days 1 and 8, every 3 weeks	155	8 (5.2)	1 (0.6)
			Cisplatin (100 mg/m^2) day 1; vinorelbine (30 mg/m^2), days 1, 8, 15 and 22, every 4 weeks	156	1 (0.6)	0
Takeda (present study)	2008	Phase III	Docetaxel (60 mg/m^2) day 8; gemcitabine (800 mg/m^2), days 1 and 8, every 3 weeks	65	8 (12.3)	3 (4.6)
			Docetaxel (60 mg/m^2) day 1, every 3 weeks	64	0 (0)	0

ILD, interstitial lung disease; TRD, treatment-related death.

benefit in patients with recurrent advanced NSCLC. The development of less toxic and more effective chemotherapeutic agents, including molecular targeted drugs, is warranted for the second-line treatment of NSCLC.

funding

Grant-in-Aid for Cancer Research from the Ministry of Health, Labour and Welfare of Japan.

acknowledgements

We thank Ms Mieko Imai for data management, Mr Takashi Asakawa, Dr Naoki Ishizuka for statistical analyses in the interim monitoring, and Dr Haruhiko Fukuda for valuable contributions to this study. This study is registered with UMIN-CTR [http://www.umin.ac.jp/ctr/index.htm umin.ac.jp/ctr], identification number C000000027].

appendix

The following institutions participated in the study: Hokkaido Cancer Center (Sapporo), Ibaragi Prefectural Central Hospital (Kasama), Tochigi Cancer Center (Utsunomiya), Nishigunma National Hospital (Shibukawa), Gunma Prefectural Cancer Center Hospital (Ohta), Saitama Cancer Center Hospital (Ina), National Cancer Center Hospital East (Kashiwa), National Cancer Center Hospital (Tokyo), International Medical Center of Japan (Tokyo), Cancer Institute Hospital (Tokyo), Toranomon Hospital (Tokyo), Kanagawa Cancer Center Hospital (Yokohama), Yokohama Municipal Hospital (Yokohama), Niigata Cancer Center Niigata Hospital (Niigata), Gifu Municipal Hospital (Gifu), Aichi Cancer Center Hospital (Nagoya), Nagoya National Hospital (Nagoya), Prefectural Aichi Hospital (Okazaki), Osaka City University Medical School (Osaka), Kinki University School of Medicine (Osaka-Sayama), Osaka Medical Center for Cancer and Cardiovascular Disease (Osaka), Osaka Prefectural Medical Center for Respiratory and Allergic disease (Habikino), Kinki-Chuo Chest Medical Center (Sakai), Toneyama National Hospital (Toyonaka), Osaka Prefectural General Hospital (Osaka), Osaka City General Hospital (Osaka), Kobe City General Hospital (Kobe), Hyogo Collage of Medicine (Nishinomiya), Hyogo Cancer Center (Akashi), Shikoku Cancer Center Hospital (Matsuyama), Kyusyu University Hospital (Fukuoka), and Kumamoto Regional Medical Center (Kumamoto).

references

1. Parkin DM. Global cancer statistics in the year 2000. Lancet Oncol 2001; 2: 533–543.
2. Dancey J, Shepherd FA, Gralla RJ et al. Quality of life assessment of second-line docetaxel versus best supportive care in patients with non-small-cell lung cancer previously treated with platinum-based chemotherapy: results of a prospective, randomized phase III trial. Lung Cancer 2004; 43: 183–194.
3. Socinski MA, Morris DE, Masters GA et al. Chemotherapeutic management of stage IV non-small cell lung cancer. Chest 2003; 123 (Suppl 1): 226S–243S.
4. Shepherd FA, Dancey J, Ramlau R et al. Prospective randomized trial of docetaxel versus best supportive care in patients with non-small-cell lung cancer previously treated with platinum-based chemotherapy. J Clin Oncol 2000; 18: 2095–2103.
5. Fossella FV, DeVore R, Kerr RN et al. Randomized phase III trial of docetaxel versus vinorelbine or ifosfamide in patients with advanced non-small-cell lung cancer previously treated with platinum-containing chemotherapy regimens: the TAX 320 Non-Small Cell Lung Cancer Study Group. J Clin Oncol 2000; 18: 2354–2362.
6. Crino L, Mosconi AM, Scagliotti G et al. Gemcitabine as second-line treatment for advanced non-small-cell lung cancer: a phase II trial. J Clin Oncol 1999; 17: 2081–2085.
7. Georgoulias V, Kouroussis C, Androulakis N et al. Front-line treatment of advanced non-small-cell lung cancer with docetaxel and gemcitabine: a multicenter phase II trial. J Clin Oncol 1999; 17: 914–920.
8. Georgoulias V, Papadakis E, Alexopoulos A et al. Platinum-based and non-platinum-based chemotherapy in advanced non-small-cell lung cancer: a randomised multicentre trial. Lancet 2001; 357: 1478–1484.
9. Hainsworth JD, Burris HA III, Billings FT III et al. Weekly docetaxel with either gemcitabine or vinorelbine as second-line treatment in patients with advanced non-small cell lung carcinoma: phase II trials of the Minnie Pearl Cancer Research Network. Cancer 2001; 92: 2391–2398.

10. Hejna M, Kornek GV, Raderer M et al. Treatment of patients with advanced nonsmall cell lung carcinoma using docetaxel and gemcitabine plus granulocyte-colony stimulating factor. Cancer 2000; 89: 516–522.
11. Kakolyris S, Papadakis E, Tsiafaki X et al. Docetaxel in combination with gemcitabine plus rhG-CSF support as second-line treatment in non-small cell lung cancer. A multicenter phase II study. Lung Cancer 2001; 32: 179–187.
12. Kosmas C, Tsavaris N, Vadiaka M et al. Gemcitabine and docetaxel as second-line chemotherapy for patients with non-small cell lung carcinoma who fail prior paclitaxel plus platinum-based regimens. Cancer 2001; 92: 2902–2910.
13. Rebattu P, Quantin X, Ardiet C et al. Dose-finding, pharmacokinetic and phase II study of docetaxel in combination with gemcitabine in patients with inoperable non-small cell lung cancer. Lung Cancer 2001; 33: 277–287.
14. Rischin D, Boyer M, Smith J et al. A phase I trial of docetaxel and gemcitabine in patients with advanced cancer. Ann Oncol 2000; 11: 421–426.
15. Spiridonidis CH, Laufman LR, Jones J et al. Phase I study of docetaxel dose escalation in combination with fixed weekly gemcitabine in patients with advanced malignancies. J Clin Oncol 1998; 16: 3866–3873.
16. Spiridonidis CH, Laufman LR, Carman L et al. Second-line chemotherapy for non-small-cell lung cancer with monthly docetaxel and weekly gemcitabine: a phase II trial. Ann Oncol 2001; 12: 89–94.
17. Kunitoh H, Watanabe K, Onoshi T et al. Phase II trial of docetaxel in previously untreated advanced non-small-cell lung cancer: a Japanese Cooperative Study. J Clin Oncol 1996; 14: 1649–1655.
18. Taguchi T, Furue H, Niitani H et al. Phase I clinical trial of RP 56976 (docetaxel) a new anticancer drug. Gan To Kagaku Ryoho 1994; 21: 1997–2005.
19. Miyazaki M, Takeda K, Ichimaru Y et al. A phase I/II study of docetaxel (D) and gemcitabine (G) combination chemotherapy for advanced non-small cell lung cancer (NSCLC). J Clin Oncol 2001; 20 (Suppl): (Abstr 2812).
20. Niho S, Kubota K, Goto K et al. Combination second-line chemotherapy with gemcitabine and docetaxel for recurrent non-small-cell lung cancer after platinum containing chemotherapy: a phase I/II trial. Cancer Chemother Pharmacol 2003; 52: 19–24.
21. Matsui K, Hirashima T, Nitta T et al. A phase I/II study comparing regimen schedules of gemcitabine and docetaxel in Japanese patients with stage IIIB/IV non-small cell lung cancer. Jpn J Clin Oncol 2005; 35: 181–187.
22. Arbuck SG, Ivy SP, Setser A et al. The Revised Common Toxicity Criteria: Version 2.0 CTEP. http://ctep.info.nih.gov (30 April 1999, date last accessed).
23. Therasse P, Arbuck SG, Eisenhauer EA et al. New guidelines to evaluate the response to treatment in solid tumors. J Natl Cancer Inst 2000; 92: 205–216.
24. Cella DF, Bonomi AE, Lloyd SR et al. Reliability and validity of the Functional Assessment of Cancer Therapy-Lung (FACT-L) quality of life instrument. Lung Cancer 1995; 12: 199–220.
25. Dunsford LM, Mead MG, Bateman CA et al. Severe pulmonary toxicity in patients treated with a combination of docetaxel and gemcitabine for metastatic transitional cell carcinoma. Ann Oncol 1999; 10: 943–947.
26. Kouroussis C, Tsavaris N, Syrigos K et al. High incidence of pulmonary toxicity of weekly docetaxel and gemcitabine in patients with non-small cell lung cancer: results of a dose-finding study. Lung Cancer 2004; 44: 363–368.
27. Pujor JL, Breton JL, Gervais R et al. Gemcitabin-docetaxel versus cisplatin–vinorelbine in advanced or metastatic non-small-cell lung cancer: a phase III study addressing the case for cisplatin. Ann Oncol 2005; 16: 602–610.
28. Ando M, Okamoto I, Yamamoto N et al. Predictive factors for interstitial lung disease, antitumor response, and survival in non–small-cell lung cancer patients treated with gefitinib. J Clin Oncol 2006; 24: 2549–2556.
29. Fukuoka M, Yano S, Giaccone G et al. Multi-institutional randomized phase II trial of gefitinib for previously treated patients with advanced non-small-cell lung cancer. J Clin Oncol 2003; 21: 2237–2246.
30. Thatcher N, Chang A, Parikh P et al. Gefitinib plus best supportive care in previously treated patients with refractory advanced non-small-cell lung cancer: results from a randomized, placebo-controlled, multicentre study (Iressa Survival Evaluation in Lung Cancer). Lancet 2005; 366: 1527–1537.
31. Pectasides D, Pectasides M, Farmakis D et al. Comparison of docetaxel and docetaxel-irinotecan combination as second-line chemotherapy in advanced non-small cell lung cancer: a randomized phase II trial. Ann Oncol 2005; 16: 294–299.
32. Wachters FM, Groen HJ, Riesma H et al. Phase II randomized trial of docetaxel vs docetaxel and irinotecan in patients with stage IIIb-IV non-small-cell lung cancer who failed first-line treatment. Br J Cancer 2005; 92: 15–20.

Int. J. Cancer: **124**, 1072–1080 (2009)

SRPX2 is overexpressed in gastric cancer and promotes cellular migration and adhesion

Kaoru Tanaka[1,2], Tokuzo Arao[1], Mari Maegawa[1], Kazuko Matsumoto[1], Hiroyasu Kaneda[1,2], Kanae Kudo[1], Yoshihiko Fujita[1], Hideyuki Yokote[1], Kazuyoshi Yanagihara[3], Yasuhide Yamada[4], Isamu Okamoto[2], Kazuhiko Nakagawa[2] and Kazuto Nishio[1]*

[1]*Department of Genome Biology, Kinki University School of Medicine, Osaka-Sayama, Osaka, Japan*
[2]*Department of Medical Oncology, Kinki University School of Medicine, Osaka-Sayama, Osaka, Japan*
[3]*Central Animal Lab, National Cancer Center Research Institute, Chuo-ku, Tokyo, Japan*
[4]*Department of Medical Oncology, National Cancer Center Hospital, Chuo-ku, Tokyo, Japan*

SRPX2 **(Sushi repeat containing protein, X-linked 2) was first identified as a downstream molecule of the *E2A-HLF* fusion gene in t(17;19)-positive leukemia cells and the biological function of this gene remains unknown. We found that *SRPX2* is overexpressed in gastric cancer and the expression and clinical features showed that high mRNA expression levels were observed in patients with unfavorable outcomes using real-time RT-PCR. The cellular distribution of SRPX2 protein showed the secretion of SRPX2 into extracellular regions and its localization in the cytoplasm. The introduction of the *SRPX2* gene into HEK293 cells did not modulate the cellular proliferative activity but did enhance the cellular migration activity, as shown using migration and scratch assays. The conditioned-medium obtained from SRPX2-overexpressing cells increased the cellular migration activity of a gastric cancer cell line, SNU-16. In addition, SRPX2 protein remarkably enhanced the cellular adhesion of SNU-16 and HSC-39 and increased the phosphorylation levels of focal adhesion kinase (FAK), as shown using western blotting, suggesting that SRPX2 enhances cellular migration and adhesion through FAK signaling. In conclusion, the overexpression of SRPX2 enhances cellular migration and adhesion in gastric cancer cells. Here, we report that the biological functions of SRPX2 include cellular migration and adhesion to cancer cells.**

Key words: SRPX2; gastric cancer; cellular adhesion; cellular migration

SRPX2 (Sushi repeat containing protein, X-linked 2) was first identified as *SRPUL* (Sushi repeat protein upregulated in leukemia) by Kurosawa *et al.*[1] The *E2A-HLF* fusion gene causes B-cell precursor acute lymphoblastic leukemia, which is characterized by an unusual paraneoplastic syndrome comprising intravascular coagulation and hypercalcemia; one of the target genes of *E2A-HLF* is *SRPX2*. Apart from the possible involvement of this gene in malignant diseases, a disease-causing mutation (p.N327S) in *SRPX2* resulting in a gain-of-glycosylation aberration in the secreted mutant protein, and the mutation actually leads to rolandic epilepsy with oral and speech dyspraxia and with mental retardation in the French family.[2] While a second mutation (p.Y72S) leads to rolandic epilepsy with bilateral perisylvian polymicrogyria in another family.[3] The involvement of *SRPX2* in these disorders suggests an important role for *SRPX2* in the perisylvian region, which is critical for language and cognitive development.

SRPX2 contains 3 sushi domains and 1 hyaline domain. A sushi domain, also known as a complement control protein module or a short complement-like repeat, contains ~60 amino acids and is found in functionally diverse proteins, such as regulators of the complement activation family, GABA receptor, thyroid peroxidase and selectin family.[4,5] Sushi domains are thought to mediate specific protein–protein or protein–carbohydrate binding and cellular adhesive functions.[4] A phylogenetic analysis revealed that *SRPX2* belongs to a family of 5 genes: *SRPX2*, *SRPX*, *SELP* (selectin P precursor), *SELE* (selectin E precursor) and *SVEP1* (selectin-like protein).[3] *SRPX/SRPX1/EXT1/DRS* has the highest degree of similarity and may be involved in X-linked retinitis pigmentosa.[6,7] The selectin family, which is well known for its biological roles in leukocyte migration, cellular attachment and rolling, also contains sushi domain repeats and are phylogenetic similar to *SRPX2*.[3]

SRPX2 also contains a hyaline (HYR) domain, and this domain probably corresponds to a new superfamily in the immunoglobulin fold. The HYR domains are often associated with sushi domains, and although the function of HYR domains is uncertain, it is thought to be involved in cellular adhesion.[8] Thus, accumulating data on the motifs found in *SRPX2* suggest that *SRPX2* may be involved in cellular adhesion.

We previously performed a microarray analysis of paired clinical samples of gastric cancer and noncancerous lesions obtained from gastric cancer patients[9] and found that *SRPX2* is overexpressed in gastric cancer tissue. The present study sought to clarify the biological function of *SRPX2* expression in gastric cancer.

Material and methods

Cell culture

HEK293 (human embryonic kidney cell line) was maintained in DMEM medium, and SNU-16, HSC-39, 44As3, HSC-43, HSC-44, MKN1 and MKN7 (human gastric cancer cell lines) were maintained in RPMI1640 medium (Sigma, St. Louis, MO) supplemented with 10% FBS (GIBCO BRL, Grand Island, NY). HUVEC (human umbilical vein endothelial cells) was maintained in Humedia-EG2 (KURABO, Tokyo, Japan) medium with 1% FBS under the addition of epidermal growth factor and fibroblast growth factor.

Expression vector construction and viral production

The full-length cDNA fragment encoding human *SRPX2* was obtained from 44As3 cells using RT-PCR and the following primers: SRPX2-F, CGG GAT CCT CAA GGA TGG CCA GTC AGC TAA CTC AAA GAG G; SRPX2-R, CCC AAG CTT GGG CTC GCA TAT GTC CCT TTG CTC CCG ACG CTG GG. The sequences of the PCR-amplified DNAs were confirmed by sequencing after cloning into a pCR-Blunt II-TOPO cloning vector (Invitrogen, Carlsbad, CA). *SRPX2* cDNA was fused to a GFP-containing pcDNA3.1 vector (Clontech, Palo Alt, CA). Empty, GFP and SRPX2-GFP vectors were then transfected into HEK293 cells using FuGENE6 transfection reagent (Roche Diagnostics, Basel, Switzerland). Hygromycin selection (100 μg/mL) was

Grant sponsors: Third-Term Comprehensive 10-Year Strategy for Cancer Control, The Program for the Promotion of Fundamental Studies in Health Sciences of the National Institute of Biomedical Innovation (NiBio), The Japan Health Sciences Foundation.

***Correspondence to:** Department of Genome Biology, Kinki University School of Medicine, 377-2 Ohno-higashi, Osaka-Sayama, Osaka 589-8511, Japan. Fax: +81-72-366-0206. E-mail: knishio@med.kindai.ac.jp

Received 18 June 2008; Accepted after revision 22 September 2008
DOI 10.1002/ijc.24065
Published online 22 October 2008 in Wiley InterScience (www.interscience.wiley.com).

performed on days 2–8 after transfection, and then the cells were cultured in normal medium for another 10 days. The vectors and stable transfectant HEK293 cells were designated as pcDNA-mock, pcDNA-GFP, pcDNA-SRPX2/GFP, HEK293-pcDNA-mock, HEK293-pcDNA-GFP and HEK293-pcDNA-SRPX2/GFP.

SRPX2 cDNA in pcDNA3.1 vector was cut out and transferred into a pQCLIN retroviral vector (BD Biosciences Clontech, San Diego, CA) together with enhanced green fluorescent protein (EGFP) following internal ribosome entry site sequence (IRES) to monitor the expression of the inserts indirectly. A pVSV-G vector (Clontech, Palo Alt, CA) for the constitution of the viral envelope and the pQCXIX constructs were cotransfected into the GP2-293 cells using FuGENE6 transfection reagent. Briefly, 80% confluent cells cultured on a 10-cm dish were transfected with 2 μg pVSV-G plus 6 μg pQCXIX vectors. After 48 hr of transfection, the culture medium was collected and the viral particles were concentrated by centrifugation at 15,000*g* for 3 hr at 4°C. The viral pellet was then resuspended in fresh RPMI1640 medium. The titer of the viral vector was calculated by counting the EGFP-positive cells that were infected by serial dilutions of virus-containing media, and the multiplicity of infection (MOI) was then determined. The viral vector and stable viral transfectant cells in each cell line were designated as pQCLIN-EGFP, pQCLIN-SRPX2, HEK293-pQCLIN-EGFP, HEK293-pQCLIN-SRPX2, MKN1-pQCLIN-EGFP and MKN1-pQCLIN-SRPX2.

Patients and samples

An analysis of *SRPX2* expression levels and clinical features was performed using data from patients aged 20 to 75 years and with histologically confirmed, Stage IV gastric cancer. Additional inclusion criteria included an Eastern Cooperative Oncology Group performance status of 0–2. The exclusion criteria included prior chemotherapy or major surgery. Fifty-seven gastric cancer samples were evaluated in this study. All the patients received chemotherapy after registration and endoscopical biopsy. Gastric cancer and noncancerous gastric mucosa samples were evaluated for *SRPX2* expression in the first consecutive 24 patients. This study was approved by the institutional review board of the National Cancer Center Hospital, and written informed consent was obtained from all the patients. Endoscopic biopsy samples were immediately placed in an RNA stabilization solution (Isogen; Nippongene, Tokyo, Japan) and stored at −80°C. Other biopsy samples obtained from the same location were reviewed by a pathologist to confirm the presence of tumor cells. The RNA extraction method and the quality check protocol have been previously described.[10]

Real-time reverse-transcription PCR

One microgram of total RNA from normal tissue purchased from Clontech and from a cultured cell line was converted to cDNA using a GeneAmp® RNA-PCR kit (Applied Biosystems, CA). Real-time PCR was carried out using the Applied Biosystems 7900HT Fast Real-time PCR System (Applied Biosystems) under the following conditions: 95°C for 6 min, 40 cycles of 95°C for 15 sec and 60°C for 1 min. Glyceraldehyde 3 phosphate dehydrogenase (*GAPD*, NM_002046) was used to normalize the expression levels in the subsequent quantitative analyses. To amplify the target genes, the following primers were purchased from TaKaRa (Yotsukaichi, Japan): SRPX2-FW, ACT GGA TTT GCG GCA TGT GA; SRPX2-RW, CCA TGT TGA AGT AGG AGC GAG TGA; GAPD-FW, GCA CCG TCA AGG CTG AGA AC; GAPD-RW, ATG GTG GTG AAG ACG CCA GT.

Anti-SRPX2 polyclonal antibody

Rabbit antibodies specific for SRPX2 were obtained by immunizing rabbits with SRPX2 peptide (FIDDYLLSNQELTQ) according to a previously described method,[2] and IgG was purified from serum using standard protocols.

SRPX2-conditioned medium

The media in which subconfluent HEK293-pQCLIN-EGFP, HEK293-pQCLIN-SRPX2, MKN1-pQCLIN-EGFP and MKN1-pQCLIN-SRPX2 cells were being cultured was replaced with a serum-reduced medium (OPTI-MEM; GIBCO), the cells were cultured for an additional 24 hr and the conditioned-media were collected. The media were filtered using Millex-GS (Millipore, Bedford, MA) and concentrated using the Amicon Ultra (Millipore) and stored at −80°C. The concentration of the conditioned-medium was measured using a BCA protein assay (Pierce Biotechnology, Rockford, IL) and equalized.

Western blot analysis

The antibodies used in this study were anti-GFP (Invitrogen, Carlsbad, CA), anti-focal adhesion kinase (anti-FAK), anti-p-FAK (pY397) (BD Biosciences), anti-β-actin (Santa Cruz Biotechnology, Santa Cruz, CA) and anti-p-FAK (pY576/577) (Cell Signaling, Beverly, MA).

A Western blot analysis was performed as described previously (Ref. 10). In brief, subconfluent cells were washed with cold phosphate-buffered saline (PBS) and harvested with Lysis A buffer containing 1%Triton X-100, 20 mM Tris-HCl (pH 7.0), 5 mM EDTA, 50 mM sodium chloride, 10 mM sodium pyrophosphate, 50 mM sodium fluoride, 1 mM sodium orthovanadate and a protease inhibitor mix, complete™ (Roche Diagnostics). Whole-cell lysates and culture medium were separated using a 2–15% gradient SDS-PAGE and blotted onto a polyvinylidene fluoride membrane. After blocking with 3% bovine serum albumin in a TBS buffer (pH 8.0) with 0.1% Tween-20, the membrane was probed with primary antibody. After rinsing twice with TBS buffer, the membrane was incubated with horseradish peroxidase-conjugated secondary antibody (Cell Signaling) and washed followed by visualization using an ECL detection system (Amersham) and LAS-3000 (Fujifilm, Tokyo, Japan). The data were quantified by automated densitometry using Multigauge Ver 3.0 (Fujifilm).The experiment was performed in triplicate.

Cellular growth assay

HEK293 transfectant cells were incubated on 96-well plates at a density of 2000/well with 180 μL of culture medium at 37°C in 5% CO_2. After 24, 48 or 72 hr of incubation, 20 μL of MTT [3-(4,5-dimethyl-thiazoyl-2-yl)2,5-diphenyltetrazolium bromide] solution (SIGMA) was added and the cultures were incubated for 4 hr at 37°C. After centrifugation, the culture medium was discarded and the wells were filled with DMSO. The absorbance of the cultures at 562 nm was measured using VERSAmax (Japan Molecular Devices, Tokyo, Japan). The experiment was performed in triplicate.

Cellular adhesion assay

EGFP-conditioned or SRPX2-conditioned media obtained from HEK293-pQCLIN-EGFP, HEK293-pQCLIN-SRPX2, MKN1-pQCLIN-EGFP or MKN1-pQCLIN-SRPX2 cells were adjusted to a concentration of 1 mg/mL and 50 μL were incubated at 4°C overnight on 96-well plates. The conditioned media were aspirated, and the wells were washed twice with PBS. The plates were then used in an adhesion assay as conditioned medium-coated 96-well plates. The cells to be analyzed were added to the wells of conditioned medium-coated plates (2×10^4 cells /well) and incubated at 37°C for 1 hr. When treated with FAK inhibitors (PP2 and Herbimycin A; Calbiochem, San Diego, CA), the cells to be analyzed were incubated for 4 hr. The wells were then washed twice with PBS to remove nonadherent cells. Adherent cells were evaluated using the MTT assay as described above. The average O.D. values of 3 wells were used for a single experiment, and the experiment was performed in triplicate.

Migration assay and chemotaxis assay

Migration assays were performed using the Boyden-chamber methods and polycarbonate membranes with an 8-μm pore size

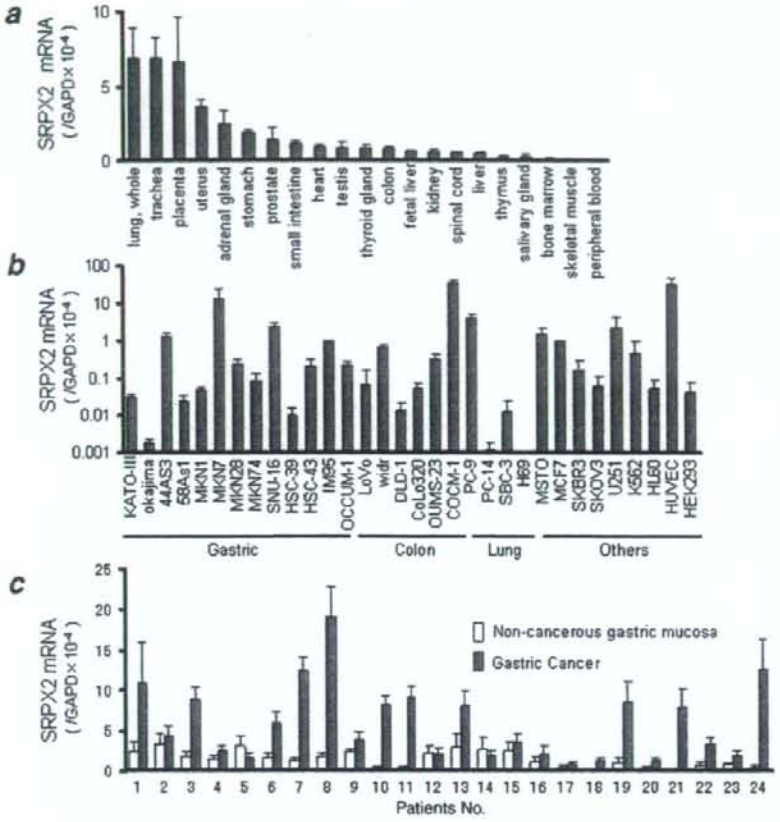

FIGURE 1 – Tissue distribution of *SRPX2* mRNA expression. The mRNA expression levels of *SRPX2* were determined using a real-time RT-PCR analysis in (*a*) human normal tissue; (*b*) 30 human cancer cell lines, HEK293 and HUVEC cell lines and (*c*) paired clinical samples that were endoscopically obtained from gastric cancer and the noncancerous gastric mucosa of the same patients. *GAPD* was used to normalize the expression levels in the subsequent quantitative analyses. The mRNA expression levels of *SRPX2* were significantly higher in the gastric cancer lesions ($p = 0.0004$). Error bars represent the SDs of 3 independent experiments. [Color figure can be viewed in the online issue, which is available at www.interscience.wiley.com.]

(chemotaxicell; KURABO). The membranes were coated with fibronectin on the outer side and dried for 2 hr at room temperature. The cells to be analyzed (2×10^4/well) were then seeded onto the upper chambers with 200 μL of migrating medium (DMEM containing 0.5% FBS), and the upper chambers were placed into the lower chambers of 24-well culture dishes containing 600 μL of DMEM containing 10% FBS. After incubation for 8 hr at 37°C, the media in the upper chambers were aspirated and the nonmigrated cells on the inner sides of the membranes were removed using a cotton swab. The cells that had migrated to the outer side of the membranes were fixed with 4% paraformaldehyde for 10 min and stained with 0.1% crystal violet for 15 min, then counted using a light microscope. The experiment was performed in triplicate.

The chemotaxis assays were performed using SNU-16 cells. A total of 1×10^5 cells were seeded onto the upper chambers with 200 μL of RPMI containing 0.5% FBS. The final concentration at 100 μg/mL of EGFP-conditioned or SRPX2-conditioned medium was added to the 600 μL volume of RPMI1640 containing 0.5% FBS medium in the lower chamber of the 24-well culture dishes. The cells were then incubated for 24 hr at 37°C with 5% CO_2. The number of migrated cells was evaluated as described earlier. The experiment was performed in triplicate.

Wound healing assay

HEK293-pQCLIN-EGFP and HEK293-pQCLIN-SRPX2 cells were plated onto 3.5-cm dishes and incubated in DMEM containing 10% FBS until they reached confluence. Wounds were introduced to the confluent cell monolayer using a plastic pipette tip. The cells were then cultured with DMEM containing 10% FBS at 37°C. After 4, 8 and 12 hr later, the wound area was photographed using a light microscope and measured. The experiment was performed in triplicate.

Fluorescent microscopy

HEK293-pcDNA-GFP and HEK293-pcDNA-SRPX2/GFP cells were treated with DAPI (6-diamidino-2-phenylindole) to stain the nucleus and photographed using fluorescent microscopy, IX71 (Olympus, Tokyo, Japan).

Statistics

The *t* test was used for comparison between 2 groups and paired *t* test was used for paired-samples in Figure 1*c*. The statistical analysis was performed using Excel software (Microsoft, Redmond, WA). A p value < 0.05 was considered significant.

Results

Tissue distribution of SRPX2 mRNA in normal tissues and cell lines

To examine the tissue distribution of *SRPX2* mRNA, we performed real-time RT-PCR for 24 normal human tissues. High expression levels of *SRPX2* mRNA were detected in the placenta, lung, trachea, uterus and adrenal gland, whereas the levels in the peripheral blood, brain and bone marrow were relatively low (Fig. 1*a*). Combined with data from previous reports,[1,2] *SRPX2* mRNA

appears to be widely observed in normal tissues, with particularly high levels detected in the placenta and lung.

SRPX2 expression was also examined in 30 human cancer cell lines, HUVEC and HEK293 cells. A relatively high *SRPX2* mRNA expression level was observed in gastric cancer (44As3, MKN7 and SNU-16), colorectal cancer (WiDr and COCM-1), lung cancer (PC-9), mesothelioma (MSTO), glioma (U251) and HUVEC. These results suggest that a variety of cancer and vascular endothelial cells express *SRPX2* (Fig. 1*b*).

TABLE I – *SRPX2* EXPRESSION AND PATIENT CHARACTERISTICS IN PATIENTS WITH GASTRIC CANCER

Characteristics	Patients No. (%)	*SRPX2* Expression (10^{-4}/*GAPD*)	*p* value
Age, years			
≥60	31 (54)	12.6 ± 12.5	0.10
<60	26 (46)	11.1 ± 9.1	
Sex			
Male	41 (72)	11.1 ± 9.1	0.61
Female	16 (28)	12.6 ± 12.5	
Histology[1]			
Diff.	22 (39)	11.3 ± 7.9	0.77
Undiff.	32 (56)	12.2 ± 11.7	
Prognosis[2]			
Favorable (≥6 months)	37 (65)	9.5 ± 7.2	<0.05
Unfavorable (<6 months)	20 (35)	15.1 ± 13.5	
Total	57		

[1]Histology of endoscopic samples divided into differentiated and undifferentiated type.–[2]Overall survival time from the first day of chemotherapy. A survival time of 6 months was used as the cut-off to divide patients into "Favorable" and "Unfavorable" groups.

Overexpression of SRPX2 mRNA in gastric cancer tissues

The expression of *SRPX2* mRNA was analyzed for paired tissues of gastric cancer and noncancerous gastric mucosa obtained from 24 gastric cancer patients. A paired *t* test demonstrated that *SRPX2* expression was significantly increased ($p = 0.0004$) in the cancerous tissues, compared to the noncancerous gastric mucosa (Fig. 1*c*). The *SRPX2* mRNA expression levels in the gastric cancer and noncancerous gastric mucosa were 6.6 ± 5.4 and 1.8 ± 1.2 ($\times 10^{-4}$/*GAPD*), respectively. Although the reason is unclear, 2 groups seemed to be present: 1 group with very high expression levels in cancerous tissues and another group with no difference in the expression levels between cancerous and noncancerous lesions.

To clarify the clinical significance of *SRPX2* expression, we examined the expression in an additional 57 gastric cancer samples using real-time RT-PCR and analyzed the correlations between *SRPX2* expression and clinical characteristics (Table I). Age, sex and histological cancer type were not correlated with *SRPX2* expression. However, patients with an unfavorable outcome, in whom the overall survival time (OS) was less than 6 months, exhibited significantly high expression levels of *SRPX2* in

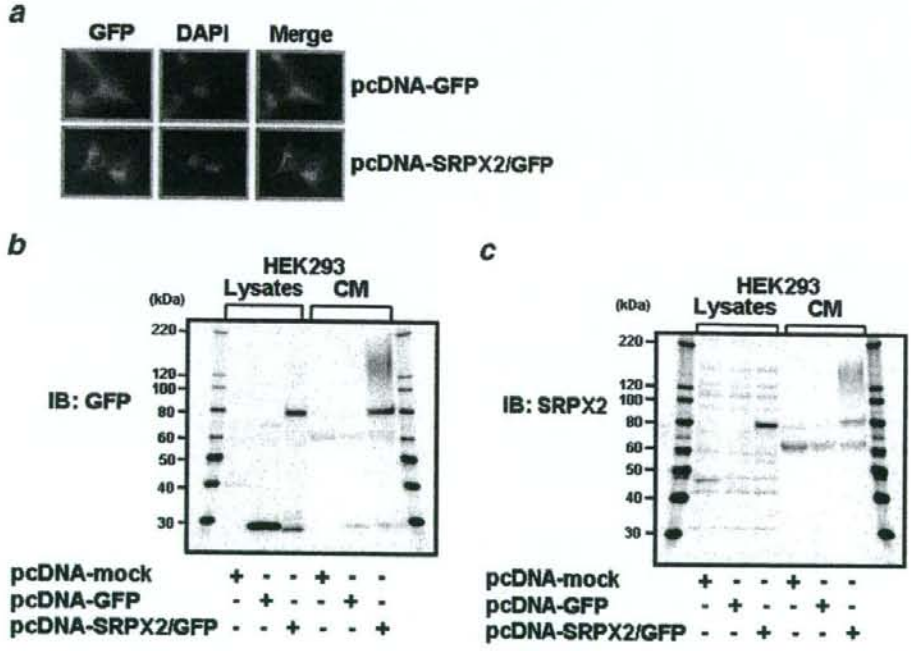

FIGURE 2 – Cellular distribution of SRPX2-GFP fusion protein. To examine the cellular distribution of SRPX2, we created cell lines expressing a fusion protein of SRPX2-GFP. The empty vector, GFP and SRPX2-GFP vectors were transfected into HEK293 cells using FuGENE6 transfection reagent. The vectors and stable transfectant cells in the HEK293 cells were designated as pcDNA-mock, pcDNA-GFP, pcDNA-SRPX2/GFP, HEK293-pcDNA-mock, HEK293-pcDNA-GFP and HEK293-pcDNA-SRPX2/GFP. (*a*) Fluorescence microscopy of HEK293-pcDNA-GFP (upper panel) and pcDNA-SRPX2/GFP cells (lower panel). The SRPX2/GFP fusion protein (green) showed a cytoplasmic distribution. The nucleus was stained by DAPI (blue). Western blot analysis detected by (*b*) anti-GFP antibody and (*c*) anti-SRPX2 antibody for HEK293-pcDNA-mock, HEK293-pcDNA-GFP and HEK293- pcDNA-SRPX2/GFP cells. Both the anti-GFP and the anti-SRPX2 antibodies detected the SRPX2-GFP fusion protein at ~80 kDa in the cell lysate and the secreted form at 150–180 kDa. IB, immunoblot; CM, culture medium.

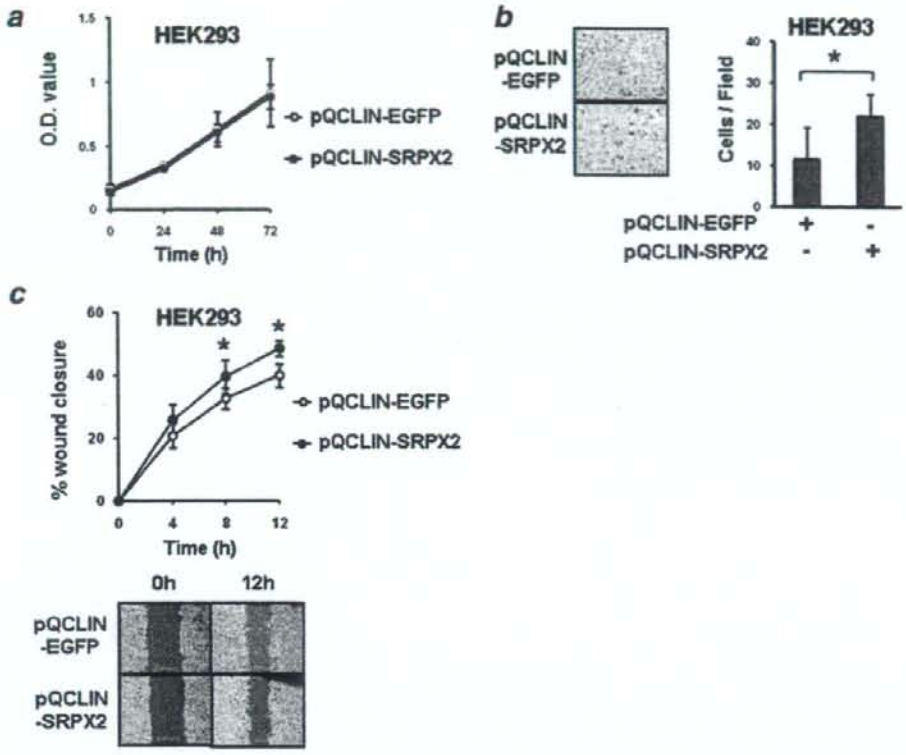

FIGURE 3 – SRPX2-introduced cells enhanced cellular migration but not cellular growth. Viral vectors containing EGFP and SRPX2 were constructed as pQCLIN-EGFP and pQLIN-SRPX2, respectively. These stable cell lines, retrovirally introduced into HEK293 cells, were designated as HEK293-pQCLIN-EGFP and HEK293-pQCLIN-SRPX2, respectively. (*a*) Cellular growth was examined using an MTT assay. No difference in cellular growth was observed between HEK293-pQCLIN-EGFP and HEK293-pQCLIN-SRPX2 cells. (*b*) Migration assay. Cells (2×10^4/well) were seeded into the upper chambers with serum-reduced medium (DMEM with 0.5% FBS). The upper chambers, with fibronectin coated on the outer side of the membrane, were then placed in the lower chambers of a 24-well culture plate containing DMEM with 10% FBS. After incubation for 8 hr at 37°C, medium was aspirated and the nonmigrated cells on the inner side of the membrane were removed using a cotton swab. The migrated cells on the outer side of the membrane were fixed, stained and counted using a light microscope. The experiment was performed in triplicate. The left panels show representative data. (*c*) Wound healing assay for HEK293-pQCLIN-EGFP and HEK293-pQCLIN-SRPX2 cells. Wounds were introduced to the confluent cell monolayer using a plastic pipette tip. After 4, 8 and 12 hr, the wound area was photographed and measured. The lower panels show representative data. The experiment was performed in triplicate. *: $p < 0.05$. EGFP, enhanced green fluorescent protein.

cancerous tissues ($p < 0.05$). The *SRPX2* expression levels in patients with an unfavorable outcome (OS < 6 months) and in those with a favorable outcome (OS > 6 months) were 9.5 ± 7.2 and 15.1 ± 13.5 ($\times 10^{-4}$/*GAPD*), respectively. This result suggests that *SRPX2* might be a prognostic biomarker, that is, associated with a malignant phenotype in gastric cancer.

SRPX2 is secreted into culture medium and localized in cytoplasm

Because the cellular distribution of an uncharacterized protein often suggest its biological function (*e.g.*, transcription factors tend to be localized in the nucleus), we tried to identify the cellular distribution of SRPX2 using a SRPX2-GFP fusion protein. We introduced an empty vector, GFP, or SRPX2 fused with GFP into HEK293 cells to create the following stable cell lines: HEK293-pcDNA-mock, HEK293-pcDNA-GFP and HEK293- pcDNA-SRPX2/GFP, respectively. The SRPX2-GFP fusion protein exhibited a cytoplasmic distribution (Fig. 2*a*). The protein expression of SRPX2 was then analyzed using western blotting and both anti-GFP and anti-SRPX2 antibodies (Figs. 2*b* and 2*c*). Western blotting with anti-GFP antibody revealed that an SRPX2-GFP fusion protein with a molecular weight (M.W.) of ~80 kDa was detected in both the cell lysates and the culture medium. A similar result was observed using anti-SRPX2 antibody. In addition, an SRPX2/GFP protein with a molecular weight of 150–180 kDa was observed in the culture medium when analyzed using both anti-GFP and anti-SRPX2 antibodies. The SRPX2 protein was detected as 2 bands with molecular weights of ~80 kDa and 150–180 kDa (containing a GFP protein of 30 kDa). The band was consistent with the estimated molecular weight of SRPX2, 53 kDa. The higher band was only observed in the culture medium and was detected using both anti-GFP and anti-SRPX2 antibodies.

SRPX2-introduced cells enhanced cellular migration but not cellular growth

To elucidate the biological function of SRPX2, EGFP or SRPX2 was retrovirally introduced into HEK293 cells. The stable cell lines were designated as HEK293-pQCLIN-EGFP and HEK293-pQCLIN-SRPX2, respectively. We then performed cellular growth assays using these cells (Fig. 3*a*). No difference in

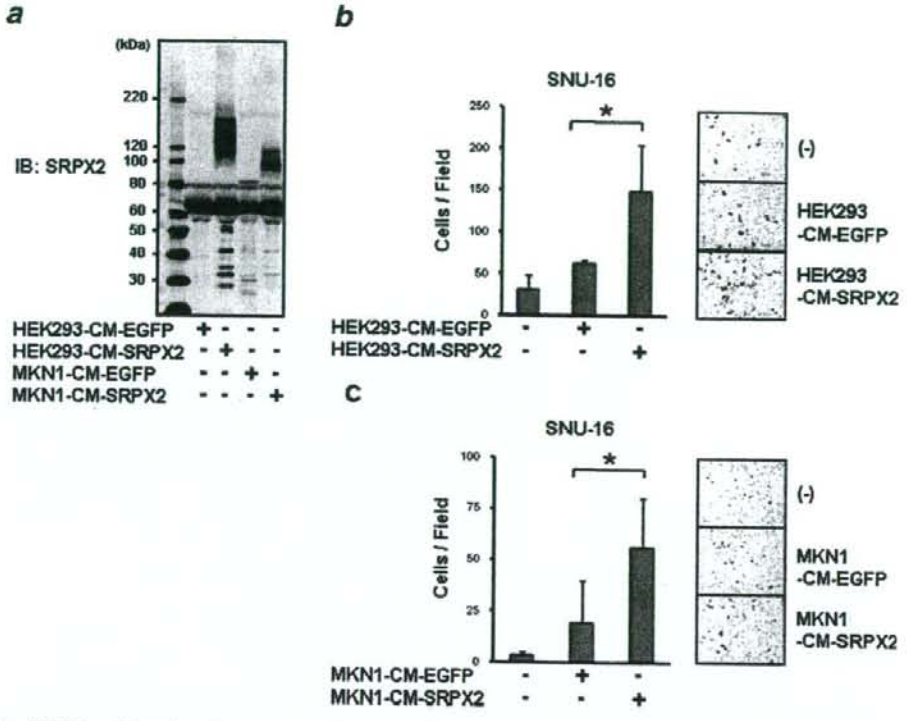

FIGURE 4 – SRPX2-conditioned medium enhanced cellular migration. (*a*) Western blotting for conditioned medium obtained from the stable cell lines, HEK293-pQCLIN-EGFP, HEK293-pQCLIN-SRPX2, MKN1-pQCLIN-EGFP and MKN1-pQCLIN-SRPX2. Each concentration of conditioned medium was adjusted to 1 mg/mL and diluted before use. Further details are described in the "Material and methods" section. IB, immunoblotting; HEK293-CM-EGFP, conditioned medium from HEK293-pQCLIN-EGFP cells; HEK293-CM-SRPX2, conditioned medium from HEK293-pQCLIN-SRPX2 cells; MKN1-CM-EGFP, conditioned medium from MKN1-pQCLIN-EGFP cells; MKN1-CM-SRPX2, conditioned medium from MKN1-pQCLIN-SRPX2 cells. The role of SRPX2 in cellular migration was assessed in the gastric cancer cell line, SNU-16, using a migration assay and EGFP- or SRPX2-conditioned medium from (*b*) HEK293-pQCLIN-EGFP or -SRPX2 cells and from (*c*) MKN1-pQCLIN-EGFP or -SRPX2 cells. A total of 1×10^5 SNU-16 cells were seeded into the upper chambers with 200 μL of RPMI containing 0.5% FBS. The final concentration of 100 μg/mL of EGFP-conditioned or SRPX2-conditioned medium was added to the 600 μL volume of the RPMI1640 containing 0.5% FBS medium in the lower chamber of the 24-well culture dish. The cells were incubated for 24 hr at 37°C. The number of migrated cells was evaluated as described earlier. The experiment was performed in triplicate. Representative data is shown in the right panels. The SRPX2-conditioned medium significantly enhanced cellular motility ($p < 0.05$) by about 2-fold, compared to the EGFP-conditioned medium. Data are shown as the mean ± SD of 3 independent experiments. *: $p < 0.05$.

cellular growth was seen between the cells, indicating that SRPX2 is not involved in cellular growth in HEK293 cells.

We next performed a migration assay to assess the role of SRPX2 in cellular motility. The cellular migration activity of the HEK293-pQCLIN-SRPX2 cells was significantly enhanced, compared to the EGFP transfectant cells ($p = 0.03$, Fig. 3*b*). A wound healing assay also demonstrated that the cellular motility of HEK293-pQCLIN-SRPX2 cells was significantly enhanced, compared to that of EGFP transfectant cells, at 8 and 12 hr after wound infliction ($p < 0.05$, Fig. 3*c*). Although the actual difference in the wound healing assay result was relatively small, these results indicate that SRPX2 is involved in cellular motility.

SRPX2-conditioned medium enhanced cellular migration

EGFP or SRPX2 was also introduced into a gastric cancer cell line, MKN1, and the SRPX2-conditioned media obtained from MKN1 and HEK293 cells were subjected to a migration assay. The transfected cells mainly produced the secreted type of SRPX2 protein with the higher molecular weight, as detected using western blot analysis. The SRPX2 proteins produced by MKN1 and HEK293 cells were observed at ~95 kDa and 110–150 kDa, respectively (Fig. 4*a*). This difference in molecular weight might be due to glycosylation.

The role of the secreted SRPX2 protein in the conditioned medium on cellular migration was assessed to SNU-16 cells using a migration assay. SNU-16 cells were incubated for 24 hr in a normal culture medium containing 100 μg/mL of EGFP- or SRPX2-conditioned medium from HEK293-pQCLIN-EGFP or -SRPX2 cells added to the lower chamber of the 24-well culture dish. The SRPX2-conditioned medium significantly enhanced the cellular motility of the SNU-16 cells ($p < 0.05$) by about 2-fold higher than that of the EGFP-conditioned medium (Fig. 4*b*). Similar results were observed using conditioned medium from MKN1-pQCLIN-EGFP or -SRPX2 cells (Fig. 4*c*). This result indicates that the secreted SRPX2 protein increased cellular motility in gastric cancer cells.

SRPX2 protein promoted cellular attachment

We examined the cellular adhesion potential of 7 gastric cancer cell lines cultured on EGFP- and SRPX2-conditioned medium-

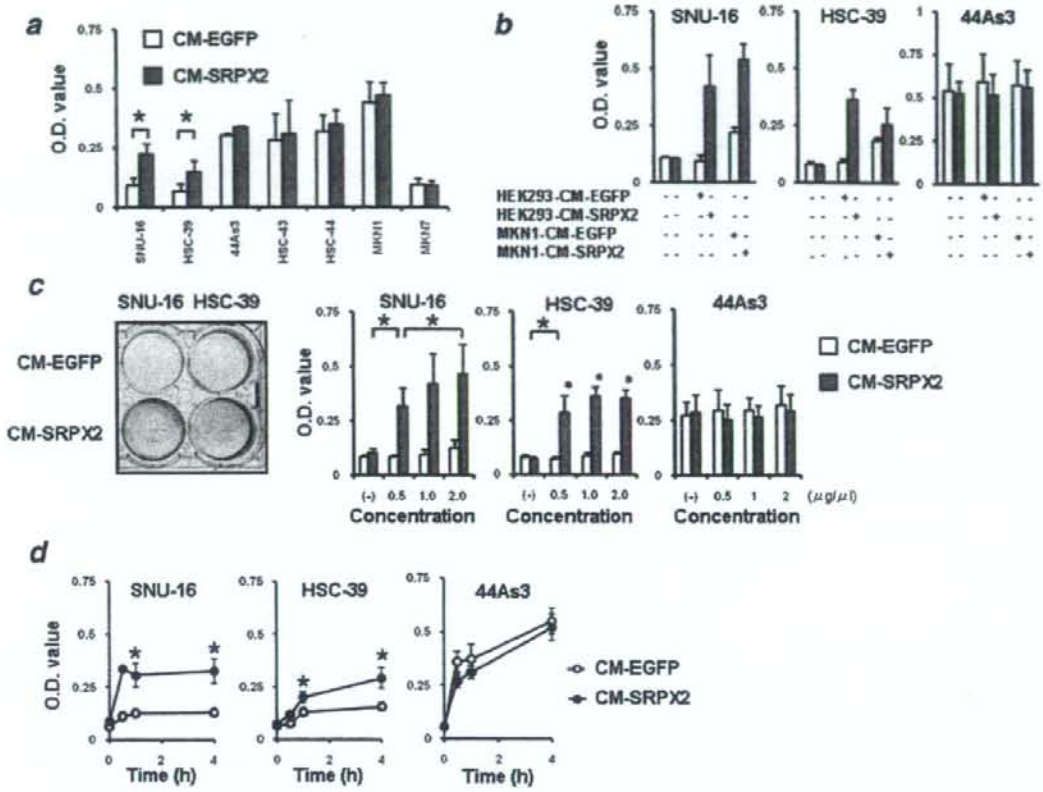

FIGURE 5 – SRPX2 protein enhanced cellular attachment. EGFP-conditioned or SRPX2-conditioned medium was adjusted to a concentration of 1 mg/mL and 50 μL was placed at 4°C overnight on 96-well plates. The conditioned medium was aspirated, and the wells were washed twice with phosphate-buffered saline (PBS). The plates were used in the adhesion assay as conditioned medium-coated 96-well plates. The cells to be analyzed (2×10^4 cells /well) were seeded into the wells of conditioned medium-coated plates and incubated at 37°C for 1 hr. The wells were then washed twice with PBS to remove nonadherent cells. The adherent cells were evaluated using an MTT assay. (*a*) A cellular adhesion assay was performed using 7 gastric cancer cell lines and conditioned medium-coated plates. The numbers of adhered SNU-16 and HSC-39 cells were significantly larger with the SRPX2-conditioned medium coated-plates ($p < 0.05$). (*b*) A cellular adhesion assay was also performed using conditioned medium-coated plates obtained from MKN1-pQCLIN-EGFP and MKN1-pQCLIN-SRPX2 cells. The numbers of adhered SNU-16 and HSC-39 cells, but not 44As3 cells, were significantly larger. (*c*) A cellular adhesion assay was performed using different concentrations of conditioned medium-coated plates. The 6-well-plate-scale data is shown in the left panel. (*d*) Cellular adhesion assay for time-course analysis. Larger numbers of attached SNU-16 and HSC-39 cells were observed from 0.5 to 4 hr. The increase in cellular attachment induced by the SRPX2 protein emerged after a relatively short time (0.5 hr). The experiment was performed in triplicate. CM-EGFP, conditioned medium from HEK293-pQCLIN-EGFP cells; CM-SRPX2, conditioned medium from HEK293-pQCLIN-SRPX2 cells. [Color figure can be viewed in the online issue, which is available at www.interscience.wiley.com.]

coated plates. Five of the gastric cancer cell lines did not increase cellular attachment to the conditioned medium-coated plate. However, the numbers of attached SNU-16 and HSC-39 cells were significantly increased by more than 2-fold by the presence of SRPX2 protein ($p < 0.05$, Fig. 5*a*).

To exclude nonspecific effects, cellular adhesion assays were also performed using conditioned medium-coated plates obtained from MKN1-pQCLIN-EGFP and MKN1-pQCLIN-SRPX2 cells (Fig. 5*b*). The SNU-16 and HSC-39 cells, but not the 44As3 cells, also exhibited a significantly larger number of adhered cells in the presence of SRPX2 protein obtained from the conditioned-medium of MKN1 cells. Cellular adhesion in these 3 cell lines was examined using 4 different concentrations of conditioned medium-coated plates. Similar results were obtained, and a dose-response effect for the conditioned medium was observed in SNU-16 cells (Fig. 5*c*). Time-course experiments revealed that a larger number of attached SNU-16 and HSC-39 cells were observed after a short time (0.5 hr) to 4 hr after the start of incubation (Fig. 5*d*). Microscopic examination revealed that most of the adhered cells did not exhibit "cell spreading" and instead resembled "cellular attachment." These results demonstrate that SRPX2 is involved in cellular attachment in SNU-16 and HSC-39 cells.

SRPX2 protein increased phosphorylation levels of FAK

FAK plays a key role in cellular adhesion, and FAK signaling is considered to be a major pathway.[11] To gain insight into the function of SRPX2, the phosphorylation levels of FAK in SNU-16 cells were examined after culturing in a medium to which SRPX2-conditioned medium had been added. Increased phosphorylation levels of FAK (pY397 and pY576/577) were observed in SNU-16 cells in the presence of SRPX2, compared to EGFP, after 1–12 hr of culture (Fig. 6*a*). FAK phosphorylation occurred during an early stage (1 hr) and was consistent with the results for cellular

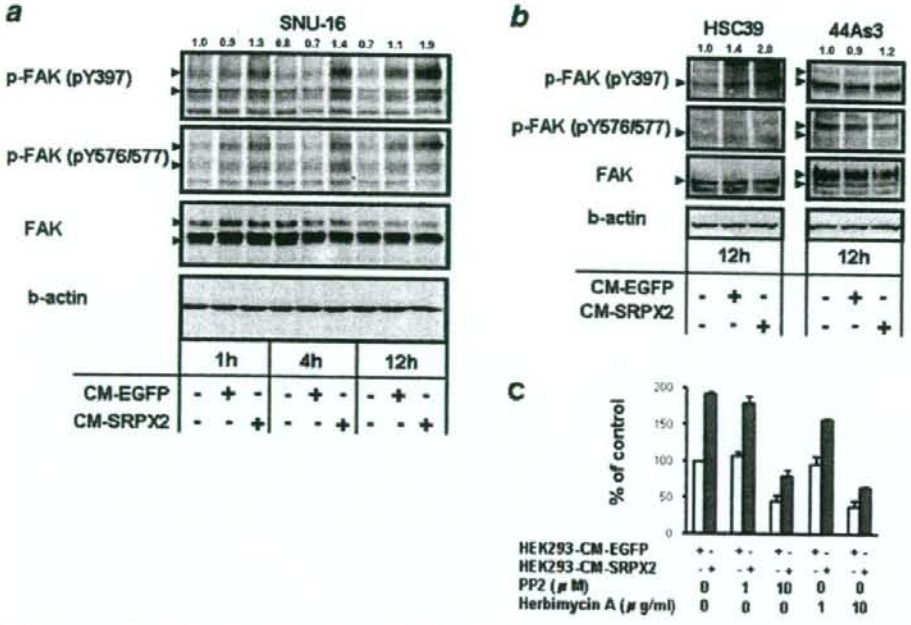

FIGURE 6 – SRPX2 protein increased the phosphorylation levels of FAK. The SNU-16 cells were cultured in RPMI with 0.5% FBS under the presence of GFP or SRPX2-conditioned medium at a final concentration of 100 μg /mL. The cells were collected at 1, 4 and 12 hr after incubation. Ten micrograms of cell lysate were subjected to western blotting using anti-phospho-FAK (pY397 and pY576/577), anti-FAK and anti-β-actin antibodies. A western blot was performed for (*a*) SNU-16 cells, and (*b*) HSC-39 and 44As3 cells. FAK, focal adhesion kinase; CM-EGFP, conditioned medium from HEK293-pQCLIN-EGFP cells; CM-SRPX2, conditioned medium from HEK293-pQCLIN-SRPX2 cells. Arrowheads: target molecules. The numerical densitometrical data of phospho-FAK (pY397) is shown above the western blot. (*c*) SNU-16 cells were treated with FAK inhibitors (PP2; final concentrations 1 or 10 μM and Herbimycin A; final concentrations 1 or 10 μg/mL) in a cellular adhesion assay to assess SRPX2-mediated attachment. Both PP2 and Herbimycin A inhibited cellular attachment of SNU-16 cells in dose-dependent manners. [Color figure can be viewed in the online issue, which is available at www.interscience.wiley.com.]

attachment. FAK phosphorylation by SRPX2 was also stimulated in HSC-39 cells but not in 44As3 cells (Fig. 6*b*). In addition, to determine whether FAK inhibitors could affect the SPRX2-mediated cellular attachment, the SNU-16 cells were treated with PP2[12] and Herbimycin A[13] to inhibit FAK activity in cellular adhesion assay (Fig. 6*c*). PP2 and Herbimycin A inhibited cellular attachment of SNU-16 cells in dose-dependent manners.

Although the molecules that transduce the extracellular SRPX2 signal into an intracellular signal remain unknown, these results suggest that the cellular phenotype caused by SRPX2 is associated with the FAK signaling pathway.

Discussion

Considering the structural features of *SRPX2*, the presence of both the sushi-repeat domain and the HYR domains predict an adhesive function.[4,8] We demonstrated that *SRPX2* enhanced cellular motility and cellular attachment, and these findings were consistent with the structural prediction.

The selectin family is the closest family to *SRPX2* and *SRPX*.[3] Selectins are known as cellular adhesion molecules and play key roles in the mediation of early neutrophil rolling on and adherence to endothelial cells.[14] Selectins recognize glycosylated proteins or lipids as their ligands, and this modification is necessary for their interaction.[15] The phylogenetical similarity between *SRPX2* and selectins suggests a similar biological function. SNU-16 and HSC-39 cells are basically nonadherent, and the increase in their cellular attachment was a relatively rapid response (0.5 hr). While number of attached cells increased significantly, the attachments were weak and the cells did not spread on the plates. Thus, the increased cellular attachment induced by SRPX2 seems to resemble neutrophil rolling.

Because the DGEA motif is a potential integrin-binding motif[16] and this motif exists in the first sushi domain of SRPX2, we hypothesized that this motif is a critical binding site for SRPX2's ability to enhance cellular migration and attachment. We examined the inhibitory effect of the DGEA peptide[16] on cell migration and attachment, but no inhibitory effect was observed (data not shown). This result suggests that the cell migration and attachment induced by SRPX2 might be independent of DGEA sequence-mediated signal transduction, or such a sequon does not function in SRPX2.

FAK is a major focal adhesion-associated protein that transmits signals downstream of integrins. FAK signals control important biological events, including cell migration, proliferation and survival, through downstream molecules like Rho, Rac, Rap1, CDC42 and PAK.[11,17,18] Our results demonstrated that SRPX2 protein increased the phosphorylation levels of FAK in SNU-16 and HSC-39 cells, but not in 44As3 cells (Figs. 6*a* and 6*b*), and enhanced the cellular adhesive potential in SNU-16 and HSC-39 cells but not in 5 other cell lines (Fig. 5*a*). We speculate that certain molecules overexpressed in SNU-16 and HSC-39 cells may localize on the cell surface and bind to SRPX2 protein, activating FAK signaling. Recently, Royer-Zemmour *et al.*[19] demonstrated the interaction of SRPX2 with uPAR (plasminogen activator, urokinase receptor) as well as with other partners such as cathepsin B. Because uPAR particularly plays an important and well-known role in various tumoral processes including cell proliferation, migration, invasion and adhesion, and because uPAR-associated

intracellular signaling may act through FAK. The SRPX2/uPAR interaction might provide a possible molecular explanation for the role of SRPX2 in cancer.

Regarding the higher fuzzy smeared-band observed in only the culture medium (Figs. 2*b*, 2*c* and 4*a*), the size of the bands differed considerably between HEK293 and MKN1 cells (110–150 kDa and ~95 kDa, respectively). These results suggest that the higher smeared bands are probably not dimmers, but they may represent a highly glycosylated protein modification. We tried to cut off the N-glycans using N-glycosidase F, but the 150-kDa smeared band did not disappear. We plan to perform additional experiments to clarify the cause of the smeared band in future studies, the results of which will undoubtedly be useful in predicting the function of SRPX2.

Many studies have indicated that selectins, the family most similar to SRPX and SRPX2 proteins, increase the interaction between tumor cells and endothelial cells, leading to tumor progression and metastasis.[20,21] Thus selectins are considered promalignancy factors.[20] Recent reports have shown that selectins positively promote angiogenesis.[22,23] Because HUVEC cells express high levels of *SRPX2* mRNA, the involvement of *SRPX2* in angiogenesis should be clarified.

In this study, we demonstrated that *SRPX2* is overexpressed in gastric cancer, compared to noncancerous gastric mucosa from the same patients, at the transcriptional level. A real-time RT-PCR analysis of 32 cell lines revealed that other cancer cells also express high levels of *SRPX2* mRNA. *SRPX2* was also overexpressed by more than 10-fold in clinical samples of colorectal cancers, compared to paired colonic mucosa (unpublished data). Thus, *SRPX2* overexpression in cancer tissue may not be restricted to gastric cancers. We plan to further examine *SRPX2* expression using immunohistochemistry in clinical samples of other cancers in the future.

Although the meaning of *SRPX2* overexpression in gastric cancer is unclear, a real-time RT-PCR analysis of clinical samples showed that *SRPX2* expression is associated with a poor prognosis in patients with gastric cancer. *SRPX2* was first identified as a downstream molecule of *E2F-HLF* in pro-B acute leukemia with t(17;19) (q23;p13) and has since been reported to contribute to malignant phenotypes.[1] *E2F-HLF*-positive leukemia is characterized by a poor outcome with bone invasion, hypercalcemia and intravascular coagulation.[24] The clinical features of leukemia and our results for gastric cancer suggest that the biological function of *SRPX2* is concerned with oncogenic activity. Further investigations of clinical outcome in relation to *SRPX2* expression are needed.

In conclusion, we found that *SRPX2* is overexpressed in gastric cancer and plays roles in cellular migration and adhesion in cancer cells. These results provide novel insight into the biological function of *SRPX2* in cancer cells.

Acknowledgements

This work was supported by funds for the Third-Term Comprehensive 10-Year Strategy for Cancer Control and the program for the promotion of Fundamental Studies in Health Sciences of the National Institute of Biomedical Innovation (NoBio) and the Japan Health Sciences Foundation. The following people have played very important roles in the conduct of this project. Miss Hiromi Orita, Dr. Hisanao Hamanaka, Dr. Ayumu Goto, Dr. Hisateru Yasui, Dr. Junichi Matsubara, Dr. Natsuko Okita, Dr. Takako Nakajima, Dr. Atsuo Takashima, Dr. Kei Muro, Dr. Takashi Ura, Miss Hideko Morita, Miss Mari Araake, Dr. Hisao Fukumoto, Dr. Tatsu Shimoyama, Dr. Naoki Hayama, Dr. Masayuki Takeda, Dr. Hideharu Kimura, Miss Kazuko Sakai, Dr. Terufumi Kato and Dr. Jun-ya Fukai.

References

1. Kurosawa H, Goi K, Inukai T, Inaba T, Chang KS, Shinjyo T, Rakestraw KM, Naeve CW, Look AT. Two candidate downstream target genes for E2A-HLF. Blood 1999;93:321–32.
2. Roll P, Rudolf G, Pereira S, Royer B, Scheffer IE, Massacrier A, Valenti MP, Roeckel-Trevisiol N, Jamali S, Beclin C, Seegmuller C, Metz-Lutz MN, et al. SRPX2 mutations in disorders of language cortex and cognition. Hum Mol Genet 2006;15:1195–207.
3. Royer B, Soares DC, Barlow PN, Bontrop RE, Roll P, Robaglia-Schlupp A, Blancher A, Levasseur A, Cau P, Pontarotti P, Szepetowski P. Molecular evolution of the human SRPX2 gene that causes brain disorders of the Rolandic and Sylvian speech areas. BMC Genet 2007;8:72.
4. O'Leary JM, Bromek K, Black GM, Uhrinova S, Schmitz C, Wang X, Krych M, Atkinson JP, Uhrin D, Barlow PN. Backbone dynamics of complement control protein (CCP) modules reveals mobility in binding surfaces. Protein Sci 2004;13:1238–50.
5. Soares DC, Gerloff DL, Syme NR, Coulson AF, Parkinson J, Barlow PN. Large-scale modelling as a route to multiple surface comparisons of the CCP module family. Protein Eng Des Sel 2005;18:379–88.
6. Meindl A, Carvalho MR, Herrmann K, Lorenz B, Achatz H, Apfelstedt-Sylla E, Wittwer B, Ross M, Meitinger T. A gene (SRPX) encoding a sushi-repeat-containing protein is deleted in patients with X-linked retinitis pigmentosa. Hum Mol Genet 1995;4:2339–46.
7. Dry KL, Aldred MA, Edgar AJ, Brown J, Manson FD, Ho MF, Prosser J, Hardwick LJ, Lennon AA, Thomson K, Keuren MV, Kurnit DM, et al. Identification of a novel gene, ETX1 from Xp21.1, a candidate gene for X-linked retintis pigmentosa (RP3). Hum Mol Genet 1995;4:2347–53.
8. Callebaut I, Gilges D, Vigon I, Mornon JP. HYR, an extracellular module involved in cellular adhesion and related to the immunoglobulin-like fold. Protein Sci 2000;9:1382–90.
9. Yamada Y, Arao T, Gotoda T, Taniguchi H, Oda I, Shirao K, Shimada Y, Hamaguchi T, Kato K, Hamano T, Koizumi F, Tamura T, et al. Identification of prognostic biomarkers in gastric cancer using endoscopic biopsy samples. Cancer Sci 2008;99:2193–99.
10. Yamanaka R, Arao T, Yajima N, Tsuchiya N, Homma J, Tanaka R, Sano M, Oide A, Sekijima M, Nishio K. Identification of expressed genes characterizing long-term survival in malignant glioma patients. Oncogene 2006;25:5994–6002.
11. Parsons JT. Focal adhesion kinase: the first ten years. J Cell Sci 2003; 116:1409–16.
12. Pala D, Kapoor M, Woods A, Kennedy L, Liu S, Chen S, Bursell L, Lyons KM, Carter DE, Beier F, Leask A. Focal adhesion kinase/Src suppresses early chondrogenesis: central role of CCN2. J Biol Chem 2008;283:9239–47.
13. Lan CC, Wu CS, Chiou MH, Hsieh PC, Yu HS. Low-energy helium-neon laser induces locomotion of the immature melanoblasts and promotes melanogenesis of the more differentiated melanoblasts: recapitulation of vitiligo repigmentation in vitro. J Invest Dermatol 2006; 126:2119–26.
14. Mousa SA. Cell adhesion molecules: potential therapeutic & diagnostic implications. Mol Biotechnol 2008;38:33–40.
15. Vestweber D, Blanks JE. Mechanisms that regulate the function of the selectins and their ligands. Physiol Rev 1999;79:181–213.
16. Mineur P, Guignandon A, Lambert ChA, Amblard M, Lapiere ChM, Nusgens BV. RGDS and DGEA-induced [Ca2+]i signalling in human dermal fibroblasts. Biochim Biophys Acta 2005;1746:28–37.
17. Schaller MD. FAK and paxillin: regulators of N-cadherin adhesion and inhibitors of cell migration? J Cell Biol 2004;166:157–9.
18. Mitra SK, Schlaepfer DD. Integrin-regulated FAK-Src signaling in normal and cancer cells. Curr Opin Cell Biol 2006;18:516–23.
19. Royer-Zemmour B, Ponsole-Lenfant M, Gara H, Roll P, Leveque C, Massacrier A, Ferracci G, Cillario J, Robaglia-Schlupp A, Vincentelli R, Cau P, Szepetowski P. Epileptic and developmental disorders of the speech cortex: ligand/receptor interaction of wild-type and mutant SRPX2 with the plasminogen activator receptor uPAR. Hum Mol Genet 2008;17:3617–30.
20. Witz IP. The selectin-selectin ligand axis in tumor progression. Cancer Metastasis Rev 2008;27:19–30.
21. Barthel SR, Gavino JD, Descheny L, Dimitroff CJ. Targeting selectins and selectin ligands in inflammation and cancer. Expert Opin Ther Targets 2007;11:1473–91.
22. Oh IY, Yoon CH, Hur J, Kim JH, Kim TY, Lee CS, Park KW, Chae IH, Oh BH, Park YB, Kim HS. Involvement of E-selectin in recruitment of endothelial progenitor cells and angiogenesis in ischemic muscle. Blood 2007;110:3891–9.
23. Egami K, Murohara T, Aoki M, Matsuishi T. Ischemia-induced angiogenesis: role of inflammatory response mediated by P-selectin. J Leukoc Biol 2006;79:971–6.
24. Hunger SP. Chromosomal translocations involving the E2A gene in acute lymphoblastic leukemia: clinical features and molecular pathogenesis. Blood 1996;87:1211–24.

Interstitial Lung Disease in Japanese Patients with Lung Cancer

A Cohort and Nested Case-Control Study

Shoji Kudoh[1], Harubumi Kato[2], Yutaka Nishiwaki[3], Masahiro Fukuoka[4], Kouichiro Nakata[5], Yukito Ichinose[6], Masahiro Tsuboi[2], Soichiro Yokota[7], Kazuhiko Nakagawa[4], Moritaka Suga[8], Japan Thoracic Radiology Group[9]*, Haiyi Jiang[10], Yohji Itoh[10], Alison Armour[11], Claire Watkins[11], Tim Higenbottam[12,13], and Fredrik Nyberg[14,15]

[1]Nippon Medical School, Tokyo, Japan; [2]Tokyo Medical University Hospital, Tokyo, Japan; [3]National Cancer Center Hospital East, Chiba, Japan; [4]Kinki University School of Medicine, Osaka, Japan; [5]Nakata Clinic, Tokyo, Japan; [6]National Kyushu Cancer Center, Fukuoka, Japan; [7]Toneyama National Hospital, Osaka, Japan; [8]Saiseikai Kumamoto Hospital, Kumamoto, Japan; [9]Japan Thoracic Radiology Group, Shiga, Japan; [10]AstraZeneca KK, Osaka, Japan; [11]AstraZeneca, Macclesfield, Cheshire, United Kingdom; [12]AstraZeneca R&D Charnwood, Loughborough, United Kingdom; [13]Sheffield University, Sheffield, United Kingdom; [14]Epidemiology, AstraZeneca R&D Mölndal, Mölndal, Sweden; and [15]Institute of Environmental Medicine, Karolinska Institute, Stockholm, Sweden

Rationale: **Interstitial lung disease (ILD) occurs in Japanese patients with non–small cell lung cancer (NSCLC) receiving gefitinib.**

Objectives: **To elucidate risk factors for ILD in Japanese patients with NSCLC during treatment with gefitinib or chemotherapy.**

Methods: **In a prospective epidemiologic cohort, 3,166 Japanese patients with advanced/recurrent NSCLC were followed for 12 weeks on 250 mg gefitinib (n = 1,872 treatment periods) or chemotherapy (n = 2,551). Patients who developed acute ILD (n = 122) and randomly selected control subjects (n = 574) entered a case-control study. Adjusted incidence rate ratios were estimated from case-control data by odds ratios (ORs) with 95% confidence intervals (CIs) using logistic regression. Crude (observed) incidence rates and risks were calculated from cohort data.**

Measurements and Main Results: **The observed (unadjusted) incidence rate over 12 weeks was 2.8 (95% CI, 2.3–3.3) per 1,000 person-weeks, 4.5 (3.5–5.4) for gefitinib versus 1.7 (1.2–2.2) for chemotherapy; the corresponding observed naive cumulative incidence rates at the end of 12-week follow-up were 4.0% (3.0–5.1%) and 2.1% (1.5–2.9%), respectively. Adjusted for imbalances in risk factors between treatments, the overall OR for gefitinib versus chemotherapy was 3.2 (1.9–5.4), elevated chiefly during the first 4 weeks (3.8 [1.9–7.7]). Other ILD risk factors in both groups included the following: older age, poor World Health Organization performance status, smoking, recent NSCLC diagnosis, reduced normal lung on computed tomography scan, preexisting chronic ILD, concurrent cardiac disease. ILD-related deaths in patients with ILD were 31.6% (gefitinib) versus 27.9% (chemotherapy); adjusted OR, 1.05 (95% CI, 0.3–3.2).**

Conclusions: **ILD was relatively common in these Japanese patients with NSCLC during therapy with gefitinib or chemotherapy, being higher in the older, smoking patient with preexisting ILD or poor performance status. The risk of developing ILD was higher with gefitinib than chemotherapy, mainly in the first 4 weeks.**

Keywords: non–small cell lung cancer; interstitial lung disease; Japanese patients; gefitinib, chemotherapy

AT A GLANCE COMMENTARY

Scientific Knowledge on the Subject

Acute interstitial lung disease (ILD) occurs in Japanese patients with non–small cell lung cancer (NSCLC) receiving gefitinib. There is, however, limited knowledge about risk factors for ILD and the incidence of ILD in patients with NSCLC receiving other treatments.

What This Study Adds to the Field

Acute ILD was common in Japanese patients with NSCLC receiving chemotherapy or gefitinib, with higher risk for gefitinib. Age, performance status, smoking, and preexisting chronic ILD were also important risk factors, aiding clinicians in treatment selection.

Epidermal growth factor receptor (EGFR) tyrosine kinase inhibitors are a well-established therapy for the treatment of non–small cell lung cancer (NSCLC) in many countries. They are generally well tolerated and not typically associated with the cytotoxic side effects commonly seen with chemotherapy.

The EGFR tyrosine kinase inhibitor gefitinib (IRESSA; AstraZeneca, London, U.K.) was first approved for the treatment of advanced NSCLC in Japan in July 2002. In clinical trials and in preapproval compassionate clinical use, some reports of interstitial lung disease (ILD)–type events had been observed. As the drug was made more widely available in Japan after approval, however, an increasing number of spontaneous reports for ILD appeared.

ILD is a disease that affects the parenchyma or alveolar region of the lungs (1). When associated with drug use, it can present precipitously with acute diffuse alveolar damage, which is fatal in some patients (2). Chest imaging shows ground-glass density and patients present with severe breathlessness. There is no specific treatment, but supportive therapy including oxygen, corticosteroids, or assisted ventilation is indicated. Acute exacerbations of ILD have previously been considered relatively rare in many settings, with Japan as a notable exception (3), but recent studies of patients with idiopathic pulmonary fibrosis (IPF) have challenged this and underlined this important risk (4).

ILD, especially IPF, is a known comorbidity in patients with NSCLC and has also been associated with many other lung cancer therapies (5). Rates of acute ILD events up to and exceeding 10% have been reported in patients receiving chemotherapy and radiotherapy (6–11). It is recognized that ILD is more common in Japan than elsewhere (5, 6, 12, 13).

(Received in original form October 11, 2007; accepted in final form March 12, 2008)

Supported by AstraZeneca.

*A list of Japan Thoracic Radiology Group members may be found in the ACKNOWLEDGMENT.

Correspondence and requests for reprints should be addressed to Fredrik Nyberg, M.P.H., M.D., Ph.D., Epidemiology, AstraZeneca R&D Mölndal, SE-413 83 Mölndal, Sweden. E-mail: fredrik.nyberg@astrazeneca.com

This article has an online supplement, which is accessible from this issue's table of contents at www.atsjournals.org

Am J Respir Crit Care Med Vol 177. pp 1348–1357, 2008
Originally Published in Press as DOI: 10.1164/rccm.200710-1501OC on March 12, 2008
Internet address: www.atsjournals.org

When safety reports of acute ILD-type events in gefitinib-treated patients appeared in Japan, there was limited knowledge about ILD in patients with NSCLC. There was a need to better understand baseline incidence on different treatments, risk factors for developing ILD, and whether gefitinib might be associated with increased risk of ILD, or if patient selection or other aspects were involved. A pharmacoepidemiologic study was designed and conducted by an independent academic team together with scientists from AstraZeneca to define the risk and increase understanding of ILD in Japanese patients with NSCLC. Some of the results of this study have been previously reported in the form of conference abstracts (14, 15).

METHODS

See also the online supplement for further details on methods.

Overall Study Design

A nonrandomized cohort study with a nested case-control study component was conducted between November 12, 2003, and February 22, 2006, in 50 centers across Japan. Patients with advanced or recurring NSCLC who had received at least one chemotherapy regimen were eligible for cohort entry. Patients and their physicians selected the most appropriate treatment (gefitinib 250 mg or chemotherapy) and the patients were followed for up to 12 weeks after treatment initiation. Basic data were collected at the start of follow-up and included sex, age, World Health Organization (WHO) performance status (PS), and tumor histology. If a patient switched to a new treatment, he or she could be re-enrolled for a new treatment period of 12 weeks, provided he or she was still eligible.

Patients who developed acute ILD events during the follow-up were registered to the case-control study nested within the cohort as clinically diagnosed potential cases. For each potential case, four patients who had not yet developed ILD were randomly selected as appropriate control subjects from patients registered to the cohort at that time, and extensive clinical and demographic risk factor data were collected on cases and control subjects (*see* Figure E1 in the online supplement).

The study followed Good Clinical Practice procedures. An independent external epidemiology advisory board provided advice on design, conduct, and analysis of the study.

Diagnosis of ILD

To ensure an accurate diagnosis of ILD, several study design components were implemented: (*1*) an information card to all cohort patients, alerting them to the symptoms of ILD; (*2*) internationally agreed criteria for the diagnosis of ILD and a diagnostic algorithm (*see* Figure E2) developed from the American Thoracic Society/European Respiratory Society consensus statement (1); and (*3*) a blinded diagnostic review of all clinically diagnosed potential ILD cases registered to the study by an independent case review board (CRB) of radiologists and clinicians.

Evaluation of Preexisting Lung Conditions

The CRB also blindly evaluated pretreatment computed tomography (CT) scans for the presence of a number of pulmonary conditions: preexisting (chronic) ILD (mainly IPF), drug-induced lung disease, pulmonary emphysema, radiation pneumonitis, lymphangitis carcinomatosis, and healed tuberculosis, and evaluated the extent of normal lung, as well as the extent of areas adherent to pleura.

Detailed Data Collection

For cases and control subjects, detailed data on NSCLC treatment, demography, cancer histology, clinical stage and the presence of metastases, WHO PS, smoking, previous cancer treatments, past and current medical history, surgical history, and concomitant medication and therapy were collected. Data on serious adverse events (SAEs) and hence all-cause mortality were collected for the gefitinib-treated patients in the cohort only; thus, information on mortality from causes other than ILD in chemotherapy-treated patients is not available from this study.

Statistical Analysis

From cohort data, we estimated observed person-time incidence rates as well as two measures of the observed "risk" of acute ILD to a patient; a naive estimate of observed cumulative incidence (incidence proportion, "frequency"), and risk up to 84 days by the Kaplan-Meier method.

Control subjects for the nested case-control study were sampled using incidence density sampling, and consequently the odds ratio (OR) obtained from the case-control analysis estimates the study incidence rate ratio (and approximately estimates the risk ratio) (16).

For the case-control statistical analysis, it was initially verified that the convenience matching for calendar time implicit in the risk set control sampling could be disregarded. In tabular analyses, we then identified potential confounders and risk factors, using as selection criteria a 10% change in the OR estimate for gefitinib versus chemotherapy treatment when stratifying for each factor separately, and a risk factor crude OR of less than 0.5 or more than 2.0, respectively. We also identified potential interactions between treatment and other risk factors, or between two potential risk factors. Modeling using logistic regression then proceeded in the corresponding four steps. Few previous data were available on risk factors for ILD in patients with NSCLC and so a hypothesis-free stepwise process with loose P value criteria ($P < 0.20$) for selection was used throughout to avoid bias.

Two sensitivity analyses were performed. First, to investigate the potential influence of the modeling approach used, a propensity score analysis was performed (17). This analysis provides an alternative way of adjusting for potential confounding bias by stratifying for a compound score based on predictors of treatment (*see* online supplement for details). Second, we estimated the possible bias due to misclassification of disease under reasonable assumptions of diagnostic error.

ILD-related mortality among the patients who developed acute ILD on gefitinib or chemotherapy treatment was obtained. Modeling of risk factors for ILD-related mortality followed a similar process to the ILD risk factor modeling. For gefitinib-treated patients, two additional data items were available: total all-cause mortality, which was analyzed by the Kaplan-Meier method, and SAEs, for which frequencies and possible consequences in terms of treatment discontinuation and death were calculated.

RESULTS

Cohort Subjects and Treatments

Cohort participation rates were high. In 10 sampled study centers, 89.6% of eligible patients were enrolled to the cohort. The number of treatment periods and subjects are summarized in Table 1. In total, 4,423 treatment periods in 3,159 subjects were available for analysis. In the cohort, 70.8% of patients had only one treatment period, 21.5% had two periods, and the remaining 7.8% of patients had three or more treatment periods registered (Table 1). Chemotherapy included a wide range of treatments, the most common being taxane monotherapy, followed by taxane+platinum and gemcitabine+vinorelbine combinations.

Cases and Control Subjects

In the overall cohort data of all treatment periods, clinicians reported 155 suspected cases of acute ILD during the follow-up, of which 122 were confirmed by the CRB after blinded review of CT and clinical data—79 of 103 gefitinib-treated (76.7%) and 43 of 52 chemotherapy-treated (82.7%) subjects. A total of 574 eligible control subjects were sampled from the person-time of the cohort. Almost all ILD cases and selected control subjects consented to participate in the nested case-control study, with final participation rates of 98.1 and 92.0%, respectively. Valid data from the CRB review of CT scans were available for 115 cases and 520 control subjects.

Descriptive Data

On data items available for the full cohort (sex, age, WHO PS, and tumor histology), the control subjects were quite represen-

TABLE 1. NUMBER OF TREATMENT PERIODS AND SUBJECTS IN THE COHORT AND NUMBER OF CASES AND CONTROLS IN THE NESTED CASE-CONTROL STUDY

	Gefitinib (*n*)	Chemotherapy (*n*)	Total (*n*)
Treatment periods registered to cohort	1,901	2,572	4,473
No treatment administered	9	15	24
Ineligible subjects	6	6	12
Protocol deviations	14	0	14
Per-protocol study cohort (treatment periods)	1,872	2,551	4,423
Subjects in cohort (first treatment periods)*	1,489	1,677	3,166
No. of subjects and order of treatment periods registered to the cohort			
1 treatment period: G			1,199
1 treatment period: C			1,036
2 treatment periods: GC			194
2 treatment periods: CG			248
2 treatment periods: CC			228
2 treatment periods: GG			9
3–8 treatment periods†: initial G			81
3–9 treatment periods‡: initial C			166
First gefitinib treatment periods total§	1,849		
Confirmed cases‖	79	43	122
Rejected cases‖	24	9	33
Control subjects	252	322	574

Definition of abbreviations: C = chemotherapy; G = gefitinib.

* Counts the first registered treatment period for each subject.

† 70% of these with three periods.

‡ 78% of these with three periods.

§ Counts the first gefitinib treatment period for all subjects with one or more gefitinib treatment registrations to the cohort; also when their very first registration was for chemotherapy.

‖ Cases registered by clinical investigators to the case-control study and subsequently confirmed or rejected by the case review board (blinded review of case diagnostic data).

tative of the overall cohort (details not shown). Comparisons of the gefitinib- and chemotherapy-treated control groups as representative of the cohort indicated that the former included more women, never-smokers, adenocarcinoma tumors, and poorer PS, as well as less preexisting ILD and pulmonary emphysema on CT scan (Tables 2 and 3). ILD cases, regardless of treatment, were more likely than cohort control subjects to be older, male, smokers, with squamous cell carcinoma histology, and have poor PS (Tables 2 and 3). The frequency of preexisting ILD and pulmonary emphysema was higher in cases, reflected also in a lower extent of normal lung on CT scan.

Cohort Analysis of ILD Occurrence

The observed incidence rate of acute ILD over the entire 12-week follow-up in the overall cohort was 2.8 per 1,000 person-weeks—4.5 in the gefitinib-treated and 1.7 in the chemotherapy subcohort (Table 4). The observed incidence in the gefitinib-treated subcohort was highest in the first 4 weeks after starting treatment, greater than in the chemotherapy-treated subcohort. In the following two 4-week periods, the incidence was lower with no clear difference (Table 4, Figure 1A). The naive cumulative incidence of ILD at 84 days (i.e., observed frequency or proportion of the original cohort that developed ILD in the study) for patients in their first study treatment period was 4.0 and 2.1% for gefitinib- and chemotherapy-treated patients, respectively (Table 4), whereas the estimated theoretical 12-week risk of ILD (i.e., taking competing causes of death and loss to follow-up into consideration; Kaplan-Meier method) was 4.5 and 2.4%, respectively (Table 4, Figure 1B). Thus, the observed cohort rates and risks suggested an association of increased ILD occurrence with gefitinib treatment mainly in the first 4 weeks after treatment initiation. All cohort estimates are unadjusted for imbalances between treatments in other risk factors. Detailed comparisons between the treatments therefore used the adjusted case-control OR (as an estimate of the adjusted incidence rate ratio) to achieve comparability.

Case-Control Analysis of ILD Occurrence and Risk Factors

Major results. The OR of developing acute ILD with gefitinib treatment versus chemotherapy, adjusted for the full predictor model of major confounders together with additional identified important risk factors and interactions, was 3.2 (95% confidence interval [CI], 1.9–5.4) (Table 5). Several risk factors aside from treatment also had strong effects, including WHO PS, as well as smoking status and preexisting ILD together with the extent of normal lung on CT scan, which interacted in a complex way in the model (Table 5, Figure 2). Preexisting ILD was confirmed as a strong risk factor, with OR point estimates ranging from 4.8 to 25.3 depending on the extent of remaining normal lung on CT scan, in comparison with patients without preexisting ILD and high extent of normal lung on CT scan (Table 5). The full set of ILD risk factors in both groups from the final model thus included older age (≥55 yr), WHO PS (≥2), smoking, short duration since NSCLC diagnosis (<6 mo), reduced extent of normal lung on CT scan (<50%), preexisting ILD, and concurrent cardiac disease. Although some potential significant interactions were seen in the initial tabular analyses (Table E1), no significant interactions with treatment (i.e., treatment-specific risk factors, or variation in treatment-related effect in subgroups defined by another risk factor) were identified in the modeling after adjustment for the relevant risk factors.

When the case-control analyses focused on the first 4 weeks after treatment initiation (because the unadjusted cohort analyses above indicated that the bulk of the association with gefitinib appeared to be for this time interval) the estimated OR adjusted for a full predictor model developed on this period's data was 3.8 (95% CI, 1.9–7.7). The same model produced an OR for Weeks 5–8 of 1.6 (95% CI, 0.5–4.8), whereas the final 4-week period had too few cases for an adequate estimate. The estimate for Weeks 5–12 combined, using this same model, was 2.5 (95% CI, 1.1–5.8). The important covariates and predictors were the same in this model as in the model for the full 12-week data, with the exception of age, preexisting cardiac disease, and preexisting pulmonary emphysema, which were not included. Due to sparse data beyond 4 weeks, independent models for Weeks 5–8, 9–12, and 5–12 could not be developed.

Confounding and sensitivity analysis. In the overall 12-week basic analysis, moderately strong confounding by other risk factors was found. The crude OR of developing ILD with gefitinib treatment versus chemotherapy was 2.3 (95% CI, 1.5–3.6). When adjusted for some of the most important potential confounders one at a time, the adjusted OR point estimate for the association of treatment with ILD occurrence ranged from 2.1 to 3.1 (*see* Table E1 for details). The most important confounder was severity of preexisting ILD with strong negative confounding, and the only one that resulted in a lower adjusted OR than 2.3 (positive confounding) was WHO PS.

The propensity score analysis approach identified the following variables as the most important predictors of selecting gefitinib treatment in this study: female sex; nonsmoking status; non–squamous tumor histology; poor PS; preexisting lymphangitis carcinomatosis; no previous gefitinib treatment; and no preexisting ILD, emphysema, or radiation pneumonitis. The

TABLE 2. CHARACTERISTICS OF CONFIRMED CASES AND CONTROL SUBJECTS (AS A RANDOM SAMPLE OF THE STUDY COHORT)

	Cases ($n = 122$)	Controls ($n = 574$)	Gefitinib Control Sample ($n = 252$)	Chemotherapy Control Sample ($n = 322$)
Sex				
Male	92 (75.4)	360 (62.7)	126 (50.0)	234 (72.7)
Female	30 (24.6)	214 (37.3)	126 (50.0)	88 (27.3)
Age				
<55 yr	11 (9.0)	95 (16.6)	43 (17.1)	52 (16.1)
≥55 yr	111 (91.0)	479 (83.4)	209 (82.9)	270 (83.9)
WHO performance status				
0	18 (14.8)	154 (26.8)	68 (27.0)	86 (26.7)
1	69 (56.6)	358 (62.4)	148 (58.7)	210 (65.2)
2–3	35 (28.7)	62 (10.8)	36 (14.3)	26 (8.1)
Histologic type				
Squamous cell carcinoma	29 (23.8)	103 (17.9)	27 (10.7)	76 (23.6)
Adenocarcinoma	80 (65.6)	414 (72.1)	207 (82.1)	207 (64.3)
Others	13 (10.7)	57 (9.9)	18 (7.1)	39 (12.1)
Smoking history				
No	21 (17.2)	192 (33.4)	113 (44.8)	79 (24.5)
Yes	100 (82.0)	382 (66.6)	139 (55.2)	243 (75.5)
Unknown	1 (0.8)	0 (0.0)	0 (0.0)	0 (0.0)
Time since diagnosis of NSCLC				
<0.5 yr	49 (40.2)	153 (26.7)	65 (25.8)	88 (27.3)
0.5 to <1 yr	36 (29.5)	154 (26.8)	67 (26.6)	87 (27.0)
>1 yr	37 (30.3)	267 (46.5)	120 (47.6)	147 (45.7)
Previous gefitinib treatment				
No	113 (92.6)	465 (81.0)	241 (95.6)	224 (69.6)
Yes	9 (7.4)	109 (19.0)	11 (4.4)	98 (30.4)
Concurrent cardiac disease				
No	111 (91.0)	556 (96.7)	244 (96.4)	312 (96.9)
Yes	11 (9.0)	19 (3.3)	9 (3.6)	10 (3.1)

Definition of abbreviations: NSCLC = non–small cell lung cancer; WHO = World Health Organization.
Values shown are numbers (%).

estimated OR of developing ILD for gefitinib treatment when stratifying by the propensity score was 3.3 (95% CI, 1.9–5.5), very similar to the primary result, suggesting that the primary regression modeling approach well captured the confounding in the data.

If some misclassification of ILD diagnosis remains despite the design features aimed to minimize it, the adjusted OR point estimate of 3.2 may apart from random variation be subject to systematic bias. A sensitivity analysis to evaluate the possible magnitude of such bias due to misclassification of ILD diagnosis suggested that the true study point estimate for the adjusted OR would be expected to lie between 2.6 and 4.8, assuming diagnostic sensitivity of more than 80% for both gefitinib- and chemotherapy-treated patients, and specificity of more than 99.0% for gefitinib and more than 99.5% for chemotherapy. Lower values for sensitivity/specificity were considered very unlikely for this serious condition in a cancer patient population, in this study setting.

Analysis of ILD Mortality

Mortality due to ILD among gefitinib- or chemotherapy-treated patients. The mortality due to ILD for the patients who developed acute ILD was 31.6% (95% CI, 21.6–43.1) among gefitinib-treated patients and 27.9% (95% CI, 15.3–43.7) among those with other treatments; the OR was 1.05 (95% CI, 0.3–3.2) for gefitinib versus chemotherapy, adjusted for relevant risk factors. Several other factors were strong predictors of a fatal outcome for patients with ILD, including age of 65 years or older, smoking history, preexisting ILD, CT scan evidence of reduced normal lung (≤50%), and/or extensive areas adherent to pleura (≥50%), with ORs ranging from 2.4 to 11.7 (*see* Table E2).

Overall mortality among gefitinib-treated patients. In the gefitinib-treated cohort in whom such data were available, an analysis of mortality from all causes by the Kaplan-Meier method showed that cumulative mortality at 12 weeks among the patients who did develop ILD was 58.7%, compared with 14.6% (95% CI, 12.8–16.3) among the large majority who did not develop ILD (Figure 3). For the entire gefitinib cohort, including the subjects who developed ILD, the observed cumulative mortality was 16.0% (95% CI, 14.3–17.8), so that the increased mortality in ILD cases impacted the total survival rate at 12 weeks in the overall gefitinib-treated cohort only to a limited extent, reducing survival from 85.4 to 84.0%.

SAEs among Gefitinib-treated Patients

SAEs were only collected for gefitinib-treated patients in the cohort, and a total of 198 patient registrations reported SAEs (10.5%), of which 38 (2.0%) reported SAEs resulting in a fatal outcome. Within this group, there were 142 patient registrations with drug-related (as reported by the physicians) SAEs (7.5%), of which 30 (1.6%) resulted in a fatal outcome. The majority of these (25 out of 30) were due to ILD-type events. There were 122 patient registrations where study treatment was discontinued due to the reported SAEs (6.5%). SAEs seen in the gefitinib-treated patients were generally consistent with the known safety profile of gefitinib and/or the patient's underlying disease and comorbidities.

DISCUSSION

This study provides important information on ILD in an advanced/recurrent NSCLC setting in Japanese patients in Japan, and it is the largest prospective study of this condition

TABLE 3. CHARACTERISTICS OF CONFIRMED CASES AND CONTROLS (AS A REPRESENTATIVE SAMPLE OF THE STUDY COHORT)

	Cases (*n* = 115)	Controls (*n* = 520)	Gefitinib Control Sample (*n* = 240)	Chemotherapy Control Sample (*n* = 280)
Severity of preexisting interstitial lung disease on CT scan (CRB evaluation)				
No ILD	84 (73.0)	473 (91.0)	231 (96.3)	242 (86.4)
Mild	15 (13.0)	28 (5.4)	8 (3.3)	20 (7.1)
Moderate	12 (10.4)	14 (2.7)	1 (0.4)	13 (4.6)
Severe	4 (3.5)	5 (1.0)	0 (0.0)	5 (1.8)
Severity of preexisting pulmonary emphysema on CT scan (CRB evaluation)				
No emphysema	56 (48.7)	326 (62.8)	176 (73.3)	150 (53.8)
Mild	35 (30.4)	92 (17.7)	36 (15.0)	56 (20.1)
Moderate	18 (15.7)	59 (11.4)	16 (6.7)	43 (15.4)
Severe	6 (5.2)	42 (8.1)	12 (5.0)	30 (10.8)
Extent of normal lung on CT scan (CRB evaluation)				
Low (10–50%)	49 (42.6)	133 (25.6)	56 (23.3)	77 (27.5)
Normal (60–100%)	66 (57.4)	387 (74.4)	184 (76.7)	203 (72.5)

Definition of abbreviations: CRB = case review board; ILD = interstitial lung disease.
Values shown are numbers (%) of total subjects with available CRB data.

to date. For the first time, the risk of acute ILD events for a large and relatively unselected chemotherapy-treated NSCLC patient cohort in Japan was determined in clinical practice. The study also quantified the greater risk of developing acute ILD associated with gefitinib treatment than with conventional chemotherapy, mainly in the first 4 weeks after treatment initiation. The study confirmed and further defined risk factors for developing ILD with gefitinib or chemotherapy. The factors included older age, poor WHO PS, smoking, short duration since diagnosis of NSCLC, reduced normal lung on CT scan, preexisting ILD, and concurrent cardiac disease. Several of these factors, or related factors, had been reported previously in bivariate or multivariate analyses from other studies (8, 18, 19). These risk factors were the same for patients treated with gefitinib or chemotherapy in the study, and no treatment-specific risk factors were identified. In particular, patients with CT evidence of preexisting ILD (chronic) were at considerably elevated risk of developing acute ILD during treatment, but there were relatively few subjects with preexisting ILD and the data did not indicate a statistically significant difference in treatment-related risk depending on the preexisting ILD status. Of clinical relevance, some of these risk factors were just as strong as, or stronger than, gefitinib treatment, for example having a poor WHO PS (≥2) rather than a good PS (OR, 4.0; 95% CI, 1.85–8.75), implying that they can be used to identify patients at particular risk of ILD in clinical practice. The relationship between ILD and pharmacokinetic characteristics of gefitinib, as well as genetic polymorphisms and proteomics determined in

TABLE 4. MEASURES OF DISEASE OCCURRENCE FOR ACUTE INTERSTITIAL LUNG DISEASE ESTIMATED FROM THE COHORT DATA (INCIDENCE RATE, CUMULATIVE INCIDENCE)

	Gefitinib Cohort	Chemotherapy Cohort
Overall observed incidence rate 0–84 d		
No. of treatment periods at Day 0	1,872	2,551
Cases of ILD/person-weeks	79/17,740	43/25,224
Incidence rate per week (95% CI)	0.00445 (0.00347–0.00544)	0.00170 (0.00120–0.00221)
Overall observed incidence rate 0–28 d		
No. of treatment periods at Day 0	1,872	2,551
Cases of ILD / person-weeks	56/7,032	21/9,902
Incidence rate per week (95% CI)	0.00796 (0.00588–0.01005)	0.00212 (0.00121–0.00303)
Overall observed incidence rate 29–56 d		
No. of treatment periods at Day 29	1,596	2,284
Cases of ILD/person-weeks	11/5,797	15/8,392
Incidence rate per week (95% CI)	0.00190 (0.00078–0.00302)	0.00179 (0.00088–0.00269)
Overall observed incidence rate 57–84 d		
No. of treatment periods at Day 57	1,328	1,890
Cases of ILD/person-weeks	12/4,911	7/6,930
Incidence rate per week (95% CI)	0.00244 (0.00106–0.00383)	0.00101 (0.00026–0.00176)
Naive cumulative incidence after 84 d (first treatment periods only)		
Cases of ILD/no. of patients	59/1,482	35/1,677
Cumulative incidence (95% CI)	3.98% (3.04–5.11%)	2.09% (1.46–2.89%)
Kaplan-Meier cumulative incidence after 84 d (first treatment periods only)		
Cases of ILD/no. of patients	59/1,482	35/1,677
Cumulative incidence (95% CI)	4.50% (3.37–5.64%)	2.40% (1.61–3.20%)

Definition of abbreviations: ILD = interstitial lung disease; CI = confidence interval.

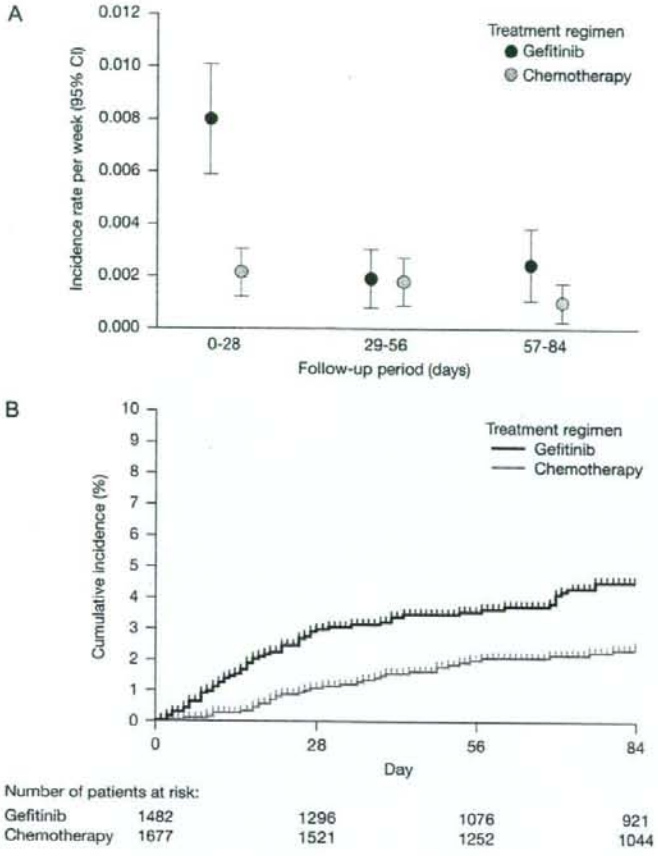

Figure 1. (*A*) Incidence rates of acute interstitial lung disease (ILD) in Japanese patients with non–small cell lung cancer for gefitinib and chemotherapy cohorts by 4-week period after treatment initiation. (*B*) Kaplan-Meier curves of risk of ILD to 12 weeks for the observed cohorts. CI = confidence interval.

study subjects, were also investigated as secondary and exploratory objectives in this study. These analyses are ongoing and results will be submitted for publication in due course.

Over the whole study follow-up, the average incidence rate for acute ILD events in patients treated with gefitinib was 3.2-fold higher relative to that seen with other chemotherapy treatments, adjusted for imbalances in other risk factors between treatments. The increased risk of ILD associated with gefitinib treatment was seen most clearly in the first 4 weeks after treatment initiation. Thus, increased physician awareness of risk factors and careful surveillance of Japanese patients during this period are indicated to manage risk. Such an approach is in line with current recommendations in Japan (20, 21). Beyond 4 weeks after treatment initiation, the risk of ILD associated with gefitinib treatment appears to fall.

ILD risk factors were found to be the same for both types of NSCLC therapy. Gefitinib is, however, a molecularly targeted agent. There is a significant body of evidence to indicate that gefitinib is a valid treatment option for some patients with NSCLC. In the IRESSA Survival Evaluation in Lung cancer (ISEL) study, a large phase III, placebo-controlled trial (n = 1,692), gefitinib was associated with some improvement in overall survival versus placebo, although this failed to reach statistical significance in the primary analysis of the overall population (22). Preplanned subgroup analyses from the study showed statistically significant differences in survival in favor of gefitinib in patients of Asian origin and those who had never smoked. Furthermore, tumor biomarker data suggest that patients with a high EGFR gene copy number, or an EGFR mutation, may be more likely to benefit (23, 24).

Therefore, the consideration of those patients more likely to benefit from the drug balanced with the better identification of these risk factors associated with ILD enables the physician to make careful judgment of the most appropriate therapy for the individual patient. Patients with several risk factors will generally be at more risk, and patients with risk factors may be at higher risk if gefitinib is used. This approach is facilitated by the fact that evidence to date suggests that subgroups less at risk of ILD tend to be those that respond well to gefitinib treatment (8).

A fatal outcome is the major concern with ILD as an SAE of drug treatment. In other large studies, fatality rates due to ILD in gefitinib-treated subjects of approximately 30% have been seen (8, 25), and a similar mortality was observed in this study in both gefitinib-treated and chemotherapy-treated ILD cases. The main predictors of a fatal outcome were older age (≥65 yr), smoking history, and preexisting ILD, as well as CT scan evidence of reduced normal lung (≤50%) or extensive areas adherent to pleura (≥50%). Because mortality is high among patients with NSCLC and the frequency of ILD in Japanese patients with NSCLC is low in comparison, ILD-related mortality impacted the overall survival at 12 weeks, for the cohort of

TABLE 5. RISK FACTORS FOR ACUTE ILD IDENTIFIED IN THE STUDY AND ESTIMATED ODDS RATIOS

Risk Factors	Odds Ratio (*95% CI*)
Treatment: gefitinib vs. chemotherapy	3.23 (1.94–5.40)
Age: ≥55 vs. ≤54 yr	1.92 (0.91–4.09)
WHO performance status	
1 vs. 0	1.57 (0.83–2.97)
2–3 vs. 0	4.02 (1.85–8.74)
Duration of NSCLC	
0.5 to <1 vs. <0.5 yr	0.65 (0.37–1.14)
≥1 vs. <0.5 yr	0.35 (0.20–0.62)
Concurrent cardiac disease: yes vs. no	2.44 (0.88–6.80)
Severity of preexisting pulmonary emphysema	
Mild vs. no	1.57 (0.89–2.79)
Moderate vs. no	1.04 (0.49–2.23)
Severe vs. no	0.47 (0.16–1.40)
Never-smoker and high extent of normal lung on CT (60–100%) (reference)	1.00 (reference)
Never-smoker and reduced extent of normal lung on CT (10–50%)	7.22 (2.52–20.64)
Smoker and high extent of normal lung on CT (60-100%)	4.43 (1.87–10.47)
Smoker and reduced extent of normal lung on CT (10–50%)	5.42 (2.08–14.12)
No preexisting ILD and high extent of normal lung on CT (60–100%) (reference)	1.00 (reference)
No preexisting ILD and reduced extent of normal lung on CT (10–50%)	7.22 (2.52–20.64)
Mild preexisting ILD and high extent of normal lung on CT (60–100%)	4.80 (1.83–12.63)
Mild preexisting ILD and reduced extent of normal lung on CT (10–50%)	6.08 (1.09–33.98)
Moderate-severe preexisting ILD and high extent of normal lung on CT (60–100%)	5.55 (1.40–21.99)
Moderate-severe preexisting ILD and reduced extent of normal lung on CT (10–50%)	25.27 (5.74–111.28)

Definition of abbreviations: CI = confidence interval; CT = computed tomography; ILD = interstitial lung disease; NSCLC = non–small cell lung cancer; WHO = World Health Organization.

gefitinib-treated patients, only to a limited extent (85.4 to 84%). Accordingly, there needs to be an appropriate individualized risk–benefit evaluation for patients also considering other treatments, many of which have their own problems with treatment-related mortality due to SAEs other than ILD.

Some methodologic issues may have influenced the study results and deserve comment. This kind of observational pharmacoepidemiologic study is generally considered sensitive to confounding by indication. Most often, it is assumed that more "sick" or "susceptible" patients will receive a new treatment,

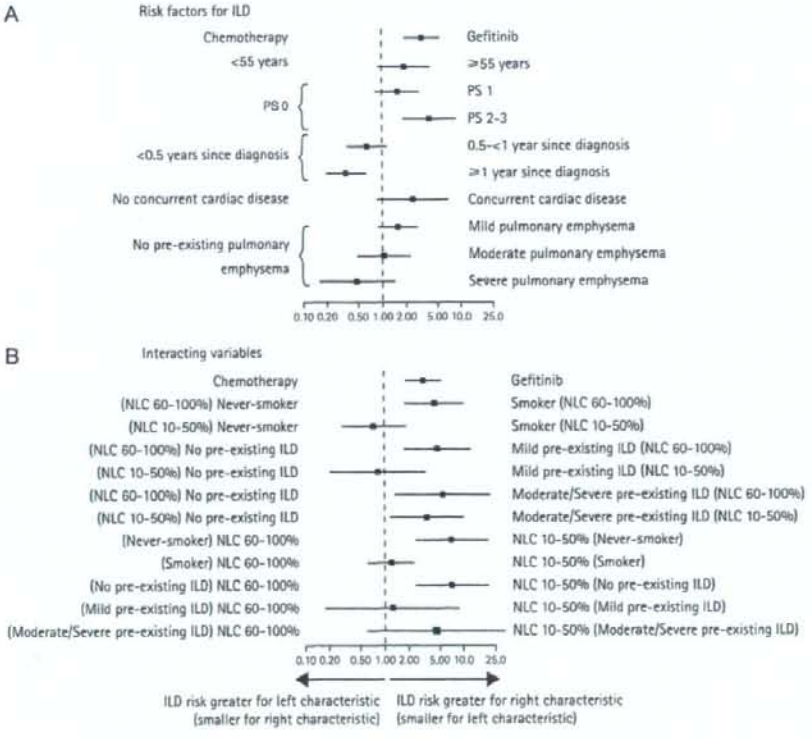

Figure 2. Adjusted odds ratios for risk factors for acute interstitial lung disease (ILD) in Japanese patients with non–small cell lung cancer from final logistic model. NLC = normal lung coverage (extent of normal lung on computed tomography scan); PS = World Health Organization performance status.

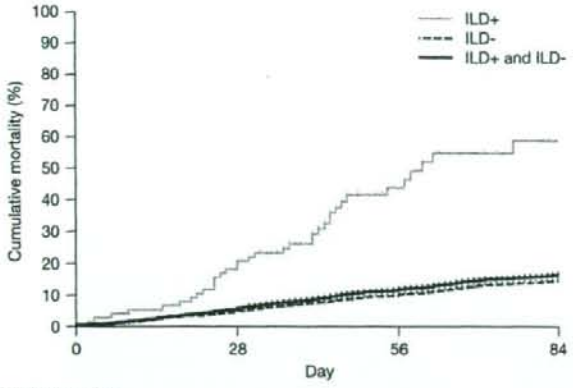

Number of patients at risk:

ILD+	78	64	22	11
ILD-	1771	1694	1416	1054
ILD+ and ILD-	1849	1758	1438	1065

Figure 3. Kaplan-Meier curves showing risk of death to 12 weeks in the gefitinib cohort overall and subdivided into those that developed interstitial lung disease (ILD+) and those who did not (ILD−).

leading to possibly more adverse effects in this group, even in the absence of a true relationship to treatment. Attempts to adjust for confounding using collected data would then push the adjusted estimate of effect closer to the null, but if sufficiently precise information on strong confounders cannot be collected, it may be impossible to remove all of the confounding. In conducting this study, the suspected adverse effect of ILD was recognized, and in the clinical setting, recommendations were in place to proceed with caution when treating some patients with suspected elevated baseline risk of ILD. This kind of selection would tend to produce the type of data pattern that was in fact observed in this study, a pattern of negative confounding that produces a more elevated OR when adjustment for confounders is performed. Thus, the results are well in line with what might be expected.

Misdiagnosis of ILD (outcome misclassification) is another concern, but it is expected that the stringent design features have minimized this problem in the present study (*see* online supplement for details). The diagnostic CRB review is a key feature, but it was still CT based, and biopsies—generally considered the gold standard for ILD diagnosis—were in most cases not taken. Overall, a sensitivity analysis suggested that, under reasonable assumptions about possible misclassification of ILD, the main result would remain similar and the conclusions from the study would not be greatly changed.

Random error is another consideration. However, although random error may be responsible for some bias in the point estimate, the confidence interval is reasonably narrow. The results are also consistent with other recent data. For example, as of January 2006, the estimated reporting rate of ILD-type events in Japan from the AstraZeneca Global Drug Safety Database of patients receiving gefitinib treatment was approximately 3.1% (26); from a retrospective study by the West Japan Thoracic Oncology Group (WJTOG), which studied 1,719 patients receiving gefitinib of whom 69 developed ILD, the frequency was 3.5% (95% CI, 2.8–4.5%) (8); from a postmarketing surveillance (PMS) study conducted by AstraZeneca KK Japan, which included 3,322 gefitinib-treated patients, it was 5.8% (25); whereas from the present study, the cumulative incidence at 12 weeks was 4.0% (95% CI, 3.0–5.1%).

These estimates are quite similar, even recognizing that the populations and selection of patients differ between these samples, and duration of follow-up, although similar, varies. In the present study, for the first time, an estimate of cumulative incidence of ILD after 12 weeks of treatment was obtained also from a chemotherapy-treated patient group; this frequency was 2.1% (95% CI, 1.5–2.9%), providing an estimate of this problem unrelated to gefitinib in patients with NSCLC in Japan.

The prognosis for gefitinib-treated patients who were diagnosed with ILD was also quite consistent with other studies. In the PMS study, ILD-related death among patients diagnosed with ILD was 38.6% (25); in the WJTOG study it was 44.3% (8); in the AstraZeneca Global Drug Safety Database as of January 2006, the proportion of ILD-type events with a fatal outcome in patients receiving treatment with gefitinib in Japan was 37.3% (AstraZeneca, data on file); and in the present study it was 31.6%. This proportion was quite similar to the chemotherapy-treated group, 27.9% (adjusted OR, 1.05; 95% CI, 0.4–3.2).

The factors associated with risk of acute ILD observed in this Japanese NSCLC population are largely different or even complementary to factors that predict better response to gefitinib. This would seem to support a hypothesis that the mechanism by which ILD occurs is distinct from the successful cancer response mechanism, offering a potential path toward selecting patients with optimal risk–benefit balance for gefitinib treatment.

Interestingly, the issue of ILD in patients with NSCLC, after gefitinib or other treatments, appears to be a problem largely limited to Japan. From the AstraZeneca Global Drug Safety Database, the reporting rate of ILD-type events in patients receiving treatment with gefitinib was only 0.23% in the rest of the world excluding Japan, based on more than 215,000 patients worldwide estimated to have been exposed to gefitinib (26). Even for neighboring countries, the pattern differs from Japan: the rate for East Asian countries, including Korea and Taiwan but excluding Japan, was 0.17% (26). The proportion of ILD-type events with a fatal outcome was similar, however: 37% in Japan and 31% in the rest of the world. The reasons for this difference in incidence of ILD between Japan and other countries remain unclear, but may relate to both constitutional and environmental factors specific to Japan or Japanese patients. For other drug treatments, too, a higher incidence of ILD has been noted in Japan than elsewhere (12, 13).

Within the study, some exploratory analyses are still ongoing related to genetic and proteomic predictors for ILD in patients with NSCLC, to search for biomarkers for early recognition of ILD and hopefully individualized risk assessment. This may

help to shed light on why ILD appears to be a particular issue for Japanese patients and the possible underlying mechanisms.

The EGFR is expressed on a number of constituent cells of the lungs including epithelium, smooth muscle cells, fibroblasts, and endothelium (27). There have been a number of animal studies using bleomycin- and vanadium pentoxide–induced lung injury with EGFR–tyrosine kinase inhibitors to determine the role of EGFR in lung fibrosis. Gefitinib and AG1478 have been used in such studies of mice and, when administered in a range of therapeutic doses, show clear attenuation of both bleomycin- (28) and vanadium pentoxide–induced (29) lung fibrosis, although one study (30) has shown augmentation of bleomycin-induced fibrosis (when using a subtoxic dose of gefitinib). The similarity of study design and choice of animal strain in the bleomycin studies make it difficult to explain the discrepant results other than by the excessive dosing. This leaves uncertainty as to the underlying mechanism of lung fibrosis in patients with NSCLC receiving gefitinib.

In summary, the study appears to be of adequate validity to avoid serious systematic biases, random error does not seem to be the most likely explanation for the results, and the observed increased risk of ILD with gefitinib treatment relative to chemotherapy treatment in Japanese patients is consistent with previous studies. Although preexisting ILD was confirmed as an important determinant of developing acute ILD symptoms after treatment with gefitinib or chemotherapy, the results also suggested that risk of ILD may be generally affected by a variety of other factors that decrease the amount of normally functioning lung tissue or affect the capability of tissue repair and recovery. The study thus identified several risk factors apart from treatment, which included preexisting ILD, which were not treatment specific, and which were partly similar to risk factors for idiopathic or rheumatic pulmonary lung fibrosis. These findings taken together suggest that there may be a common etiology that gives some patients a greater susceptibility both to idiopathic or rheumatic pulmonary fibrosis and to acute drug-induced lung injury after various treatments.

Conflict of Interest Statement: S.K. does not have a financial relationship with a commercial entity that has an interest in the subject of this manuscript. H.K. does not have a financial relationship with a commercial entity that has an interest in the subject of this manuscript. Y.N. does not have a financial relationship with a commercial entity that has an interest in the subject of this manuscript. M.F. does not have a financial relationship with a commercial entity that has an interest in the subject of this manuscript. K.N. does not have a financial relationship with a commercial entity that has an interest in the subject of this manuscript. Y.I. does not have a financial relationship with a commercial entity that has an interest in the subject of this manuscript. M.T. does not have a financial relationship with a commercial entity that has an interest in the subject of this manuscript. S.Y. does not have a financial relationship with a commercial entity that has an interest in the subject of this manuscript. K.N. does not have a financial relationship with a commercial entity that has an interest in the subject of this manuscript. M.S. does not have a financial relationship with a commercial entity that has an interest in the subject of this manuscript. The Japan Thoracic Radiology Group does not have a financial relationship with a commercial entity that has an interest in the subject of this manuscript. H.J. has been an AstraZeneca employee since 2001. Y.I. has been an AstraZeneca employee since 2000. A.A. is a full-time employee of AstraZeneca. C.W. has been a full-time employee at AstraZeneca since 2001 until present and owns shares in the company. T.H. is a full-time R&D scientist at AstraZeneca, UK, and received stock options. F.N. is a full-time employee of AstraZeneca and owns shares in the company.

Acknowledgment: The authors thank the study monitors, nurses, data managers, other support staff, and the patients participating in the study; the external epidemiology advisory board (Kenneth J. Rothman, Jonathan M. Samet, Toshiro Takezaki, Kotaro Ozasa, Masahiko Ando) for their advice and scientific review of study design, conduct, and analysis; Professor Nestor Müller for his expert input into radiologic aspects of ILD diagnosis; all case review board members (including Japan Thoracic Radiology Group members [with *]) individually (Moritaka Suga, Takeshi Johkoh*, Masashi Takahashi*, Yoshiharu Ohno*, Sonoko Nagai, Yoshio Taguchi, Yoshikazu Inoue, Takashi Yana, Masahiko Kusumoto*, Hiroaki Arakawa*, Akinobu Yoshimura, Makoto Nishio, Yuichiro Ohe, Kunihiko Yoshimura, Hiroki Takahashi, Yukihiko Sugiyama, Masahito Ebina, and Fumikazu Sakai*) for their valuable work in blindly reviewing ILD diagnoses, as well as prestudy CT scans for preexisting comorbidities; and all hospitals and clinical investigators who contributed to the data collection in the study (*see below*). The authors thank Sarah Charlesworth, from Complete Medical Communications, who provided editing assistance funded by AstraZeneca.

Hospitals and principal investigators contributing to the study: National Hospital Organization Hokkaido Cancer Centre (Hiroshi Isobe), Hokkaido University Hospital (Koichi Yamazaki), National Hospital Organization Dohoku National Hospital (Yuka Fujita), Tohoku University Hospital (Akira Inoue), Sendai Kousei Hospital (Shunichi Sugawara), National Cancer Centre Hospital East (Yutaka Nishiwaki), Nippon Medical School Chiba Hokusoh Hospital (Yasushi Ono), Tokyo Medical University Hospital (Masahiro Tsuboi), Nippon Medical School Hospital (Tetsuya Okano), Toho University Omori Medical Centre (Nobuyuki Hamanaka), Toranomon Hospital (Kunihiko Yoshimura), National Hospital Organization Tokyo Hospital (Atsuhisa Tamura), Juntendo University Hospital (Kazuhisa Takahashi), Kyorin University Hospital (Tomoyuki Goya), Tokai University Hospital (Kenji Eguchi), Kitasato University School of Medicine (Noriyuki Masuda), Kanagawa Cardiovascular and Respiratory Centre (Takashi Ogura), Niigata Cancer Centre Hospital (Akira Yokoyama), National Nishi-Niigata Central Hospital (Hiromi Miyao), Toyama University Hospital (Muneharu Maruyama), Kanazawa University Hospital (Kazuo Kasahara), Aichi Hospital, Aichi Cancer Centre (Hiroshi Saito), National Hospital Organization Nagoya Medical Centre (Hideo Saka), Fujita Health University Hospital (Hiroki Sakakibara), Nagoya Ekisaikai Hospital (Masashi Yamamoto), Shiga University of Medical Science Hospital (Noriaki Tezuka), Kyoto Katsura Hospital (Takeshi Hanawa), National Hospital Organization Kyoto Medical Centre (Yoshiyuki Sasaki), Rinku General Medical Centre Municipal Izumisano Hospital (Hisao Uejima), Kinki University, School of Medicine (Kazuhiko Nakagawa), National Hospital Organization Kinki-chuo Chest Medical Centre (Masaaki Kawahara), Osaka City General Hospital (Koji Takeda), Osaka City General Hospital (Hirohito Tada), Osaka City University Hospital (Shinzoh Kudoh), Osaka Prefectural Medical Centre for Respiratory and Allergic Diseases (Kaoru Matsui), Osaka Police Hospital (Kiyoshi Komuta), Toneyama National Hospital (Soichiro Yokota), Kobe City General Hospital (Keisuke Tomii), Hyogo Medical Centre for Adults (Shunichi Negoro), Kobe University Hospital (Yoshihiro Nishimura), Institute of Biomedical Research and Innovation (Nobuyuki Katakami), Tenri Hospital (Yoshio Taguchi), Okayama University Medical and Dental School Hospital (Katsuyuki Kiura), Hiroshima City Hospital (Hidetaka Sumiyoshi), Hiroshima City Hospital (Noritomo Senoo), National Hospital Organization Shikoku Cancer Centre (Tetsu Shinkai), National Hospital Organization Kyushu Cancer Centre (Yukito Ichinose), Fukuoka National Hospital (Akira Motohiro), University of Occupational and Environmental Health (Masamitsu Kido), University of Occupational and Environmental Health (Kenji Sugio), National Hospital Organization Nagasaki Medical Centre (Akitoshi Kinoshita), Kumamoto University Hospital (Mitsuhiro Matsumoto), Kumamoto-Chuo Hospital (Sunao Ushijima), Okinawa National Hospital (Mutsuo Kuba).

References

1. American Thoracic Society. American Thoracic Society/European Respiratory Society international multidisciplinary consensus classification of the idiopathic interstitial pneumonias. *Am J Respir Crit Care Med* 2002;165:277–304.
2. Inoue A, Saijo Y, Maemondo M, Gomi K, Tokue Y, Kimura Y, Ebina M, Kikuchi T, Moriya T, Nukiwa T. Severe acute interstitial pneumonia and gefitinib. *Lancet* 2003;361:137–139.
3. Kondoh Y, Taniguchi H, Kawabata Y, Yokoi T, Suzuki K, Takagi K. Acute exacerbation in idiopathic pulmonary fibrosis: analysis of clinical and pathologic findings in three cases. *Chest* 1993;103:1808–1812.
4. Wells AU, Hogaboam CM. Update in diffuse parenchymal lung disease 2006. *Am J Respir Crit Care Med* 2007;175:655–660.
5. Raghu G, Nyberg F, Morgan G. The epidemiology of interstitial lung disease and its association with lung cancer. *Br J Cancer* 2004;91:S3–S10.
6. Kudoh S, Takeda K, Nakagawa K, Takada M, Katakami N, Matsui K, Shinkai T, Sawa T, Goto I, Semba H, *et al.* Phase III study of docetaxel compared with vinorelbine in elderly patients with advanced non-small-cell lung cancer: results of the West Japan Thoracic Oncology Group Trial (WJTOG 9904). *J Clin Oncol* 2006;24:3657–3663.
7. Abid SH, Malhotra V, Perry MC. Radiation-induced and chemotherapy-induced pulmonary injury. *Curr Opin Oncol* 2001;13:242–248.
8. Ando M, Okamoto I, Yamamoto N, Takeda K, Tamura K, Seto T, Ariyoshi Y, Fukuoka M. Predictive factors for interstitial lung disease, antitumor response, and survival in non-small-cell lung cancer patients treated with gefitinib. *J Clin Oncol* 2006;24:2549–2556.
9. Danson S, Blackhall F, Hulse P, Ranson M. Interstitial lung disease in lung cancer: separating disease progression from treatment effects. *Drug Saf* 2005;28:103–113.
10. Rossi SE, Erasmus JJ, McAdams HP, Sporn TA, Goodman PC. Pulmonary drug toxicity: radiologic and pathologic manifestations. *Radiographics* 2000;20:1245–1259.
11. Sandler AB, Nemunaitis J, Denham C, von Pawel J, Cormier Y, Gatzemeier U, Mattson K, Manegold C, Palmer MC, Gregor A, *et al.* Phase III trial of gemcitabine plus cisplatin versus cisplatin alone in patients with locally